



**eo clinic**  
the wall-in satellite support



# COVID-19 Impact on Agricultural Practices in Moldova

## Work Order REPORT

Supporting:

United Nations Development Programme (UNDP)





---

Products elaborated in EO CLINIC activity are realized to the best of our ability, optimizing the available data and information.

All geographic information has limitations due to scale, resolution, date and interpretation of the original sources. No liability concerning the contents or the use thereof is assumed by the producer and by the ESA.

Deliverables produced by ITHACA and Mallon Technology released by e-GEOS.

© ESA, on request by **UNDP Moldova**.

© design/layout - **Ion Axenti**, 2020

# TABLE OF CONTENTS

**LIST OF FIGURES .....4**

**LIST OF TABLES .....6**

**ABOUT THIS DOCUMENT .....7**

**ABOUT THE EO CLINIC.....7**

**AUTHORS .....7**

**ACKNOWLEDGEMENTS .....8**

**1. Development Context and Background .....9**

**2. Proposed Work Logic for EO-Based Solutions ..... 10**

    2.1 Service 1: Cropland Distribution and Status .....10

    2.2 Service 2: Mobility Trends to Reveal Agricultural Practice Anomalies.....11

**3. Delivered Eo-Based Products and Services ..... 16**

**3.1 Service 1: Cropland Distribution and Status .....16**

        3.1.1 Specifications..... 16

        3.1.2 Quality Control and Validation .....23

        3.1.3 Usage, Limitations and Constraints.....24

**3.2 Service 2: Mobility Trends to Reveal Agricultural Practice Anomalies.....24**

        3.2.1 Specifications.....24

            3.2.1.1 Analysis and evaluation of status of orchards in 2020 season..... 16

            Mapping of orchard distribution..... 16

        3.2.2 Quality Control and Validation .....44

        3.2.3 Usage, Limitations and Constraints.....49

**3.3 WEBGIS publication.....50**

## LIST OF FIGURES

Figure 1: Diagram of NDVI/time and possible derived phenological parameters .....	12
Figure 2: Arable land map for 2017 over the AOI. The confidence values are assigned based on temporal consistency checks. Masked areas are in white.....	17
Figure 3: Season Start, Peak, End and maximum Greenness for the 2018 over the AOI. ....	18
Figure 4: Outline of season characterization method for Season Start Peak and End.....	19
Figure 5: Season Peak comparison from year 2017 (top left) to 2020 (bottom right).....	20
Figure 6: Maximum Greenness comparison from year 2017 (top left) to 2020 (bottom right).....	21
Figure 7: Average monthly time series over the station of Falesti (data is provided by the website "Reliable Prognosis", rp5.ru, and made available by the Moldova UNDP representative).....	22
Figure 8: Average maximum greenness for each Raion.....	22
Figure 9: Total arable land for each Raion.....	23
Figure 10: Harvesting Evidence confidence for the 2018 over the AOI.....	24
Figure 11: In the figure an example of orchard regular pattern visible on the orthophoto.....	25
Figure 12: On the left the typical pattern of vineyard based on equally spaced rows of grapevines. On the right a photo of the identified vineyard visible on Google Earth.....	26
Figure 13: Orchard distribution divided into districts. ....	26
Figure 14: Example of spatial distribution of orchards in Falesti district. Orchards have been distinguished between residential and not residential. Residential orchard are localised within or closed to urban areas. ....	29
Figure 15: Test areas identified in the AOI in order to check the complete procedure for seasonal NDVI function fitting and phenological parameters extraction.....	30
Figure 16: Examples of Start Of Season (left image) and Mid Of Season (right image) phenological parameter maps produced from Sentinel-2 NDVI time-series (pixel level, only orchard areas are represented in map) for the 2019 vegetation growing season.....	31
Figure 17: Examples of maps of seasonal Amplitude (right image) and Length (left image) phenological parameters produced from Sentinel-2 NDVI time-series (pixel level, only orchard areas are represented in map) for the 2019 vegetation growing season.....	31
Figure 18: Examples of statistical metrics evaluated at orchard level for each growing season in the time-series 2017-2020 and for all the examined phenological parameters. In the example in figure, statistical metrics refer only to the Start of Season and Seasonal Small Integral parameters evaluated in the 2019 growing season and to the orchard polygon highlighted in yellow circle.....	32

Figure 19: Examples of statistical metrics evaluated at orchard level for each growing season in the time-series 2017-2020 and for all the examined phenological parameters.....32

Figure 20: Example of map of the Seasonal Small Integral (SMI) phenological parameter produced at pixel level (left image, outputs are produced in raster format) and orchard level.....33

Figure 21: Examples of maps showing the spatial distribution of the Start of Season shifts (on the left) and of the percent deviations of the Seasonal Small Integral parameter (on the right) for the 2020 vegetation growing season respect to reference average values observed in 2017-2019 seasons, evaluated at pixel level.....35

Figure 22: Example of classification at orchard level for 2020 Seasonal Small Integral parameter deviations.....35

Figure 23: Examples of maps showing the classes of deviation for the Start of Season shifts and of the percent deviations of the Seasonal Small Integral parameter parameters evaluated for the 2020 growing season respect to reference average values observed in 2017-2019 seasons, produced at orchard level.....36

Figure 24: Density population in 2019 in the area of interest. Added pie charts show the distribution of the population in rural and urban (left), and under, in and over working age (right). .....37

Figure 25: Density population for 2015 in the area of interest, derived by GHSL data is shown on the left. The right image shows the GHSL population aggregated by municipalities. ....38

Figure 26: Heatmap representing the distribution of the 112-emergency service call, registered as suspicious cases of covid-19. Left figure shows the Moldova situation. The situation in the AOI is shown on the right. ....39

Figure 27: Distribution of the total calls to 112, normalised by population and classified from 1 to 5 score.....40

Figure 28: Trend of the 112 emergency calls by day, aggregated by month for the rayons in the Area of Interest. ....41

Figure 29: 112-emergency service calls registered as suspicious cases of Covid-19, normalised on population and classified by percentiles, and aggregated by municipalities.....42

Figure 30: Distribution of the rate possible affected crops (left) and orchards (right), respect to the total crops and orchards area.....43

Figure 31: On the left, the final score obtained to evaluate the general deviation of the vegetation status respect to the lasts years. On the right the summary index which aim to link the previous index with the one calculated for the 112-emergency calls analysed.....44

Figure 32: Mean number of Sentinel-2 monthly good observation in a year from 2017 to 2019. ....46

Figure 33: Example of QA layer for year 2019.....46

## LIST OF TABLES

Table 1:	Types of orchards identified within the area of interest.....	27
Table 2:	Table summarizing the examined phenological parameter values, temporally and spatially integrated over all the orchard polygons belonging in the AOI, according to an average rule. ....	33
Table 3:	Distribution in the whole AOI of the deviations of Seasonal Small Integral and Start Season phenological parameters for the 2020 growing season respect to average values (2017-2019), evaluated at orchard field level.....	36
Table 4:	Distribution of agricultural areas by rayon.....	37
Table 5:	Total calls and population in absolute numbers, average of the normalised calls on GHSL population. ....	39
Table 6:	Percent area distribution of monthly good observations in orchard areas, during the period of analysis (Jan 2017-May 2020) - yearly analysis. ....	45
Table 7:	Percent area distribution of monthly good observations in orchard areas, during the period of analysis (Jan 2017-May 2020) - monthly analysis.....	45
Table 8:	Distribution of validation points. ....	47
Table 9:	Confusion matrix.....	47
Table 10:	Classification accuracies and errors.....	48
Table 11:	Population from 2019 and 2015 by rayon and variation between 2015 and 2019.....	48
Table 12:	Covid-19 cases from ESRI online dashboard platform of Moldova.....	49

## ABOUT THIS DOCUMENT

This publication was prepared in the framework of the EO Clinic (Earth Observation Clinic, see below), in partnership between ESA (European Space Agency), the United Nations Development Programme (UNDP) and team of service providers contracted by ESA: e-GEOS S.p.A. as Prime with support from Mallon Technology Ltd and ITHACA.

This Work Order Report (WOR) describes the context of the activities on COVID-19 Impact on Agricultural Practices in Moldova, the geoinformation requirements of the activities and finally, the EO products and services delivered by the EO Clinic service providers in support of those activities.

## ABOUT THE EO CLINIC

The EO Clinic (Earth Observation Clinic) is an ESA (European Space Agency) initiative to create a rapid-response mechanism for small-scale and exploratory uses of satellite EO information in support of a wide range of International Development projects and activities. The EO Clinic consists of “on-call” technically pre-qualified teams of EO service suppliers and satellite remote sensing experts in ESA member states. These teams are ready to demonstrate the utility of satellite data for the development sector, using their wide range of geospatial data skills and experience with a large variety of satellite data types.

The support teams are ready to meet the short delivery timescales often required by the development sector, targeting a maximum of 3 months from request to solution.

The EO Clinic is also an opportunity to explore more innovative EO products related to developing or improving methodologies for deriving socio-economic and environmental parameters and indicators.

The EO Clinic was launched in March 2019 and is open to support requests by key development banks and agencies during the 2 years project duration.

## AUTHORS

The present document was prepared and coordinated by Valeria Donzelli (Project manager, e-GEOS) with support from the following contributors: Paul Farrell (Technical Manager, Mallon Technology Ltd), Andrea Melchiorre (Senior Engineer – Thematic expert, Mallon Technology Ltd), Polyanne Aguiar (Senior Engineer – Thematic Expert, Mallon Technology Ltd.), Francesca Perez (Technical Manager, ITHACA), Franca Disabato (Senior Engineer - Thematic expert, ITHACA), Cristina Monaco (Senior Engineer - Thematic expert, ITHACA).

## ACKNOWLEDGEMENTS

The following colleagues provided valuable inputs, insights and evaluation feedback on the work performed: Dumitru Vasilescu (Policy Specialist, UNDP), Danu Marin (UNDP), and Zoltan Bartalis (ESA Coordinator and Technical Officer)..

### FOR FURTHER INFORMATION

Please contact Valeria Donzelli (Project manager, e-GEOS, [valeria.donzelli@e-geos.it](mailto:valeria.donzelli@e-geos.it)) with copy to [Zoltan.Bartalis@esa.int](mailto:Zoltan.Bartalis@esa.int) if you have questions or comments with respect to content or if you wish to obtain permission for using the material in this report.

Visit the ESA EO Clinic: [https://eo4society.esa.int/eo\\_clinic](https://eo4society.esa.int/eo_clinic).



# 1. Development Context and Background

The United Nations Development Programme (UNDP) and the Moldovan Government are merging efforts to create a national collaborative platform for new evidence, to include satellite Earth Observation (EO), big data (in particular on mobility) and other types of data in a multi-layered platform with multiple points and levels of access and visualisation of core products at national level, with the possibility to zoom in at the most granular level.

Service 1 aimed at contributing to the monitoring of the agricultural product on and the estimation of the impact of COVID-19 on the local agricultural practices. The goal was to provide additional evidence on the recent events investigating historical and current EO observations over the four *raion* of Falesti, Ungheni, Balti and Singerei.

The work focus area was on arable land. Crop specific studies require additional data and information on location and type of crops grown. For this reason, the service aimed to identify arable land versus, non-vegetated and forested areas. Over arable land, growing season parameters (start, peak, end) and maximum greenness was analysed at the Sentinel 2 spatial resolution (10 m). Results were also aggregated at *raion* (district) level to demonstrate the possibility of scaling up the service results at national scale.

Service 2 activities are devoted to highlight possible spatial correlation between Covid-19 impact on population and anomalies detected on vegetation, with a particular focus on the vegetative state of orchards, which are examined in the first phase of Service 2, and of cropped areas, which are examined in Service 1. For this purpose, information about the 2020 vegetation status in orchard area are evaluated and, together with the similar one provided for cropped areas as outcome of Service 1 activities, will be exploited in the subsequent activity aimed at analysing Covid-19 trends to support the identification of agricultural areas impacted.



## 2. Proposed Work Logic for EO-Based Solutions

The project has included two services:

- Service 1 – Cropland Distribution and Status
- Service 2 – Mobility Trends to Reveal Agricultural Practice Anomalies

The approach for the development and implementation of each these services are described in the following sections.

### 2.1 Service 1: Cropland Distribution and Status

Service 1 goal was to identify arable crop areas based on maximum greenness and growth season. The analysis of the years 2017 – 2019 was used as baseline for comparing 2020 data.

Service 1 is based on Copernicus/ESA Sentinel 2 Multi-Spectral Imager (MSI) data. The datasets were pre-processed to Surface Reflectance (L2A) to reduce atmospheric effects. The Scene Classification layer was used to remove clouds, shadows, water and snow-covered pixels. Different vegetation indices were used to estimate the maximum greenness and crop growth season start, peak and end.

The analysis was performed on pre-processed time series of vegetation indices, the Normalized Difference Vegetation Index (NDVI) was used as a proxy of greenness to derive peak season, the Normalized Difference Red Edge (NDRE) was used to estimate the growing season start month and the Normalized Burn Ratio 2 (NBR2) for harvesting month.

Name	Equation	Use
Normalized Difference Vegetation Index (NDVI)	$NDVI = \frac{\rho_{NIR} - \rho_{Red}}{\rho_{NIR} + \rho_{Red}}$	Arable land mask, Peak Season, Max Greenness
Normalized Difference Red Edge (NDRE)	$NDRE = \frac{\rho_{NIR} - \rho_{re1}}{\rho_{NIR} + \rho_{re1}}$	Arable land mask, Season Start
Normalized Burn Ratio 2 (NBR2)	$NBR2 = \frac{\rho_{Swir2} - \rho_{Swir1}}{\rho_{Swir2} + \rho_{Swir1}}$	Arable land mask, Season End

Season characterization is based on the analysis of the vegetation indices time series shape and variations (drops/ increases).

The output is a map of arable crop land containing three different values of confidence: High, Medium, and Low. Confidence values were estimated using temporal consistencies checks of the vegetation indices indicators. A secondary confidence layer is generated for harvesting detection. For each year considered the maximum greenness, growth season start, peak and end date maps were also generated.

## 2.2 Service 2: Mobility Trends to Reveal Agricultural Practice Anomalies

In Service 2, as regards the identification of areas where fruit tree evolution for the 2020 growing season show some modifications respect to 2017-2019 previous seasons, considered as reference conditions, two different activities are proposed, as described in the following. This information, together with the one provided for cropped areas as outcome of Service 1 activities, was exploited together with the outcomes of the activities devoted to the analysis of call phones to 112 emergency service, in order to investigate and possibly model the relationships between vegetation conditions and the diffusion of suspicious cases related to Covid-19 in the examined AOI. Unfortunately the unavailability of CDR data prevented from the analysis of this information and its correlation with vegetation anomalies.

The spatial distribution of orchards in the AOI has been identified and mapped by means of computer-aided photo interpretation (CAPI) techniques carried out on very high resolution orthoimagery (2016) available in the Moldova geospatial portals. Refinement and validation activities have been carried out, according to the approaches described in 3.2.2.

The activity of characterization of orchards fields in the AOI is aimed at identifying the fundamental phenological stages of vegetation starting from the analysis of a properly selected vegetation index dataset derived from available satellite imagery. For this purpose, the following steps have been carried out:

- 1. NDVI archive creation.** NDVI data has been extracted from Sentinel-2 Level 2A BOA reflectance imagery and the proper NDVI time-series spanning from January 2017 to May 2020 has been created on a pixel basis. Temporal composite images have been used for this purpose. The final time frequency of observations in time-series, suitable for correctly support the subsequent analyses, has been selected based on a preliminary investigation about cloud persistence in Sentinel-2 imagery covering in the AOI. For this purpose, Sentinel-2 decadal and monthly image composites properly obtained from the Sentinel-2 Global Mosaic (S2GM) service have been analysed. According to this analysis (see 3.2.2), monthly NDVI time-series have been produced.

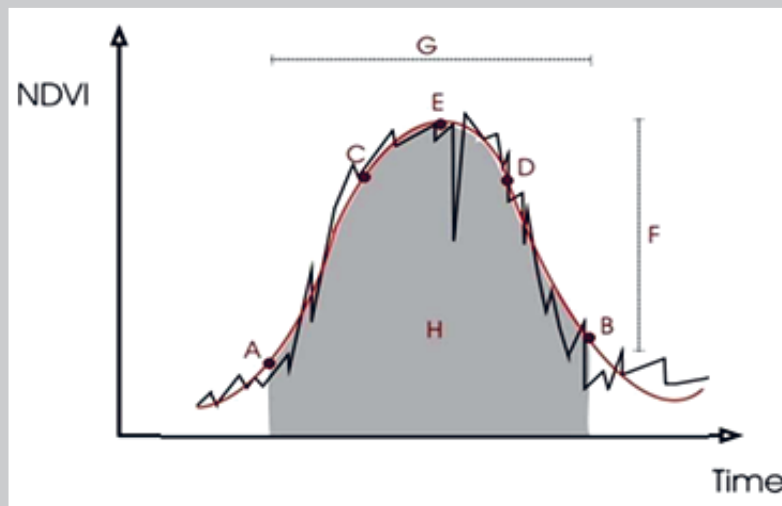
**2. NDVI time-series modelling** with smoothed and continuous functions from which phenological parameters are extracted. Proposed modelling operations include:

- detection and removal of spikes, residual noise reduction through a median filtering operation;
- gap filling;
- NDVI time-series modelling. The modelling phase involves two different steps: the initial determination of the number of the yearly phenological cycles in the NDVI time-series, and NDVI time-series fitting. The phenological cycles identified are locally interpolated using a properly selected least-squares fitting algorithm. The proposed local fitting procedure is based on a asymmetric gaussian functions.

Data quality information provided together with base Sentinel-2 composite imagery has been incorporated in this phase and used to differently filter observations during NDVI time-series gap filling and modelling operations.

**3. Phenological parameters extraction.** Seasonal changes observed in NDVI time-series generally have proven to be useful in tracking land surface phenology and vegetation development stages, providing insights into key cropping events such as planting, harvesting, and growing period. For the purpose of this study, for each phenological cycle modelled on a pixel basis, some phenological parameters (see A-F in Figure 1) are extracted from the satellite-derived modelled NDVI function.

Figure 1: **Diagram of NDVI/time and possible derived phenological parameters**



(A-F; for instance, A=Start of the Season (modelled from satellite imagery); B=End of the Season; H=Seasonal Small Integral; G=Length of the Season; F=Amplitude of the Season) for a sample vegetation growing season..

In particular, following phenological parameters, extracted from the fitted NDVI time-series for the vegetated pixels, have been taken into consideration for orchard area characterization in AOI:

- Start Of Season (SOS) parameter: the Day Of the Year (DOY), mapped at pixel level;
- Length Of Season (LOS, n. of days), computed as difference between EOS and SOS;

- Seasonal Amplitude, computed as  $(NDVI_{max} - NDVI_{min})$ ;
- Time for the mid of the season (MID), computed as the mean value of the times for which, respectively, the left edge has increased to the 80 % level and the right edge has decreased to the 80 % level.
- Small seasonal integral (SMI), computed as the integral of the local interpolated NDVI temporal profile within SOS and EOS and mapped at pixel level.

Estimation of SOS (in terms of DOY) are based on a user defined VI thresholding approach (20% of the seasonal amplitude, measured from the left/right minimum level).

Phenological parameters have been extracted and mapped originally at pixel level, that is, at the original spatial resolution of examined Sentinel-2 imagery (10 m) and further summarized for each orchard field in the AOI.

Starting from obtained results, a further activity devoted to map the 2020 orchard status in AOI is carried out. In this activity, for selected phenological parameter, positive and negative deviations respect to the historical normal behaviour (evaluated using the 2017-2019 time-series) are calculated at a pixel level and mapped. Deviations are then evaluated and mapped at orchard level selecting a proper classification schema, and considering a maximum frequency approach for the identification of the final deviation class and type to be assigned to each orchard in the AOI. The analysis of deviations allows the detection, in the whole AOI, of orchard areas affected by modified conditions in the 2020 vegetation growing season. These areas can be interpreted, with more caution, as possibly areas where fruit tree evolution and condition for the 2020 growing season is different from previous years and, therefore, potentially affected by the Covid-19 spread. Caution is needed because the proposed methodology does not allow distinguishing the actual causes of the observed deviations, also due, for example, to different climatic conditions in the observed years (i.e. temperature, rain, frost), or land cover changes. In particular, for the purposes of proposed monitoring activities, two phenological parameters are considered as fundamental in order to characterize the analysed vegetation growing seasons: the Start of the Season (SOS) and the Seasonal Small Integral (SMI). These parameters are able to describe synthetically the trend of the season in both the time and the integrated NDVI/time domains and are generally well correlated with the seasonal vegetation productivity.

In the following section, the methodology applied on **ancillary data** in order to evaluate the possible correlation between vegetation deviation in 2020 and Covid-19 spread in the AOI is described.

Input data available for the AOI are the ones downloadable by the web site of Moldova Statistics. Most of this data are only at national level, so not useful for a detailed analysis over the AOI, as information about the workforce and agricultural sector. Other data aggregated at district level has been evaluated not adequate for the delineation of the population distribution in the AOI.

In order to cope with this issue, other public dataset have been explored. The Global Human Settlement Layer (GHSL) from 2015 that gives a population count distributed on 250m cell has been taken into account. This data has the required level of spatial granularity but is old in term of temporal update.

The other interesting input data given are the single call to the 112-emergency service are available, for the whole country. The calls are collected on a 91 days data range (from 16/03/2020 to 14/06/2020), for a total of 13680 records. This is a subset of the calls

in Moldova

to 112-emergency service, related only to suspect Covid-19 cases, but only 184 calls explicitly report symptoms of upper respiratory tract (27 inside the AOI). The calls are geolocated through a hexagonal grid (12 986 cells), which covers the whole Moldova.

The given hexagonal grid also contains information about municipalities and has been used as reference to aggregate data by municipalities, as no other source of information about municipality boundaries were available (OSM data was incomplete).

The calls to 112 has been aggregated by space and time, in particular:

- Selection of calls inside the AOI;
- Total count of the call, aggregated on single hexagonal grid of the AOI and on municipalities;
- Monthly count of the calls, aggregated on municipalities.

As the distribution of values is affected by the presence of urban areas, the data has been be weighted on population data, in order to highlight where number of calls have been higher respect to population. In order to preserve the adequate level of spatial granularity, it has been decided to use GHSL 2015 data. Considering the population as homogeneously distributed over a GHSL cell, data has been re-aggregated on the hexagonal grid.

In addition, a normalisation of data has been applied, in order to better compare the call and population data. The comparison (normalised call over normalised population) has been performed only at municipality level, has there was some inconsistencies between datasets at single grid level (e.g. grid with call where no population is available).

A scoring system has been attributed to normalised call evaluating the percentiles distribution of values, in order to have a scoring system from 1 to 5, where 5 indicated high impact of the calls respect to the population.

The final step of the proposed work was to perform some mobility analysis in order to identify anomalies in patterns and support the identification of priority areas and to help the proper interpretation of final obtained results and models. The anonymized call detail records (CDR) for the years 2017–2020 were essential to this contribution, because this set represented the only type of data from which it possible to extract mobility patterns, as no other source of information about traffic and people movement is available for the area. As no data about mobility is finally available, 112 emergency calls have been used as a proxy for Covid-19 hotspot and a spatial correlation between calls distribution and vegetation distribution has been performed.

For crops information, a mask extracted by selecting zone with high level of confidence from the output produced in Service 1 has been used. Between products, the crop mask referred only to 2019 has been chosen. This mask has also been refined excluding some urban areas, used in Service 2 for the orchard detection, and orchard areas, produced in Service 2, which overlays crops areas.

For crops anomalies, areas that in 2020 which are no more detected as crops, as from the output given by service 1, have been used. The mask has been only refined on 2019 crop mask previously refined, in order to maintain consistency between masks. For each municipality, the extension in term of area (square km) of crops and no more crops area has been calculated and the rate of no more crops area on crops area in 2019 has been used as parameter to evaluate the situation between municipalities.

A similar operation has been performed on orchards areas, derived in Service 2. The

orchards validated have been used to calculate the total area of orchards for each municipality and the orchards showing a negative deviation for the Seasonal Small Integral (SMI) parameter in the 2020 growing season have been used to estimate the areas with a possible deviation in the vegetation conditions. The rate between orchards area with negative deviation and total orchard area has been used as parameter to evaluate the situation between municipalities.

The final step was the comparison between observed deviation in vegetation by municipality and the calls to 112 normalised on population and aggregated by municipalities.

The rates of negative deviation by municipality have been classified evaluating their percentile distribution. The final score for crops and orchards is represented by the sum of the score obtained for each municipality. This value represents the evaluation of deviation in vegetation status for the 2020. The sum of this final value on vegetation with the one obtained on the 112 calls, want to represent areas where high anomalies in vegetation are related with high numbers of calls to emergency services, representing a possible areas where the correlation between the two events may be possible.



## 3. Delivered EO-Based Products And Services

### 3.1 Service 1: Cropland Distribution and Status

#### 3.1.1. Specifications

##### Historic Period 2017 - 2019

Service 1 outputs were generated using Sentinel 2 MSI data and a land cover layer.

Necessary input data:

- At least 1 cloud-free Sentinel 2 acquisition in 5 different months of a given year
- Static land cover layer (e.g. Copernicus Global Land Cover)

Optional input data:

- Yearly updated land cover layer
- Cadastral Units
- Crop type farmed

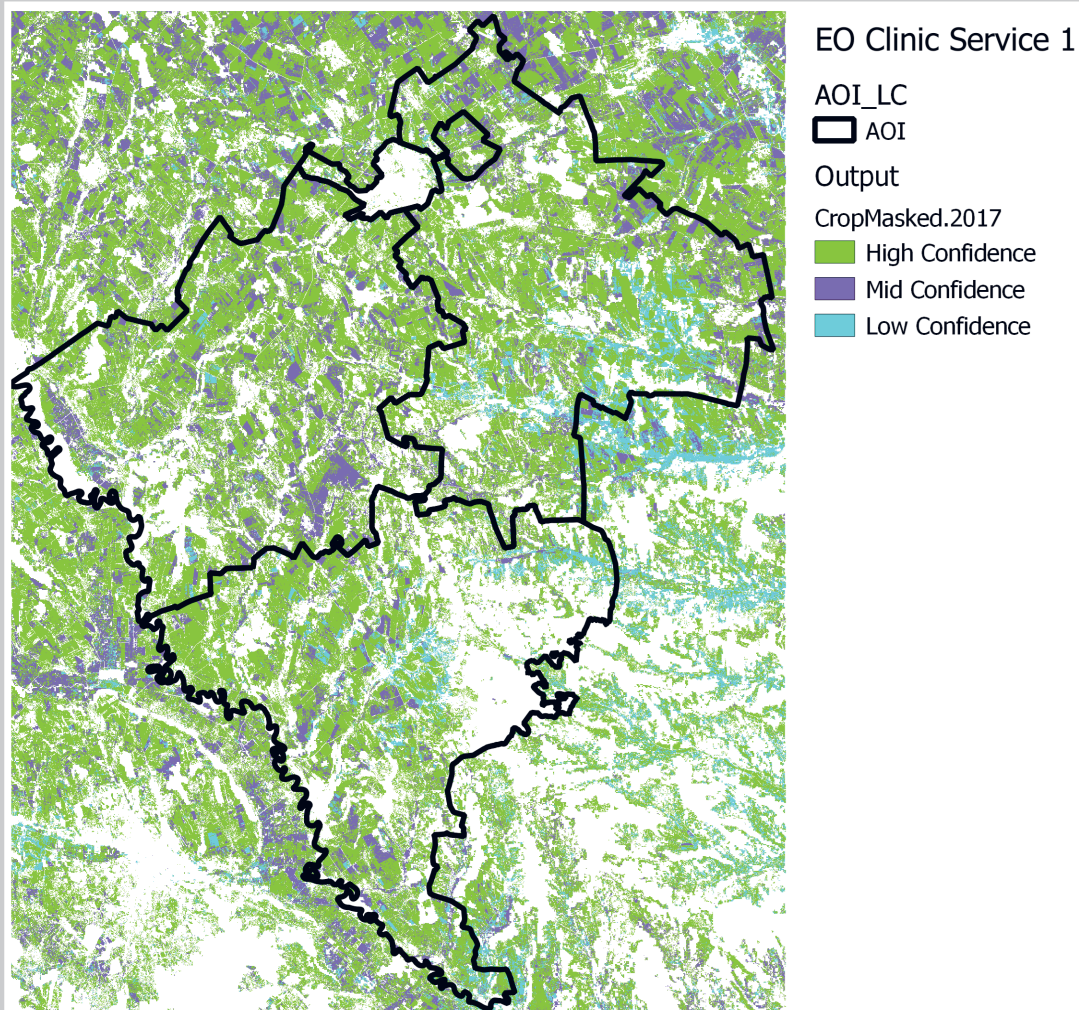
The **Land cover raster layer** is necessary to have a preliminary masking of agricultural areas. The accuracy of the land cover layer has a direct impact on the output accuracy, however further refinements are operated using Sentinel 2 data.

An **arable crop mask** is generated using different criteria:

1. Land cover class agricultural area
2. Evidence of vegetated area
3. Evidence of forested area

The arable crop mask is built to minimize omission errors and excludes urban and forested area. Temporal consistency checks are used to highlight higher confidence arable land areas (Figure 2). A further layer is provided indicating harvesting evidence probability (further information in section 3.1.2)

Figure 2: Arable land map for 2017 over the AOI. The confidence values are assigned based on temporal consistency checks. Masked areas are in white



Cadastral units and crop type information can additionally be used to stratify the analysis per different crop. If these data are available the arable crop mask can be used to visualize areas not cultivated within the parcels and fully characterize the cadastral units at object level (i.e., considering statistics of all the pixels falling within the parcel footprint).

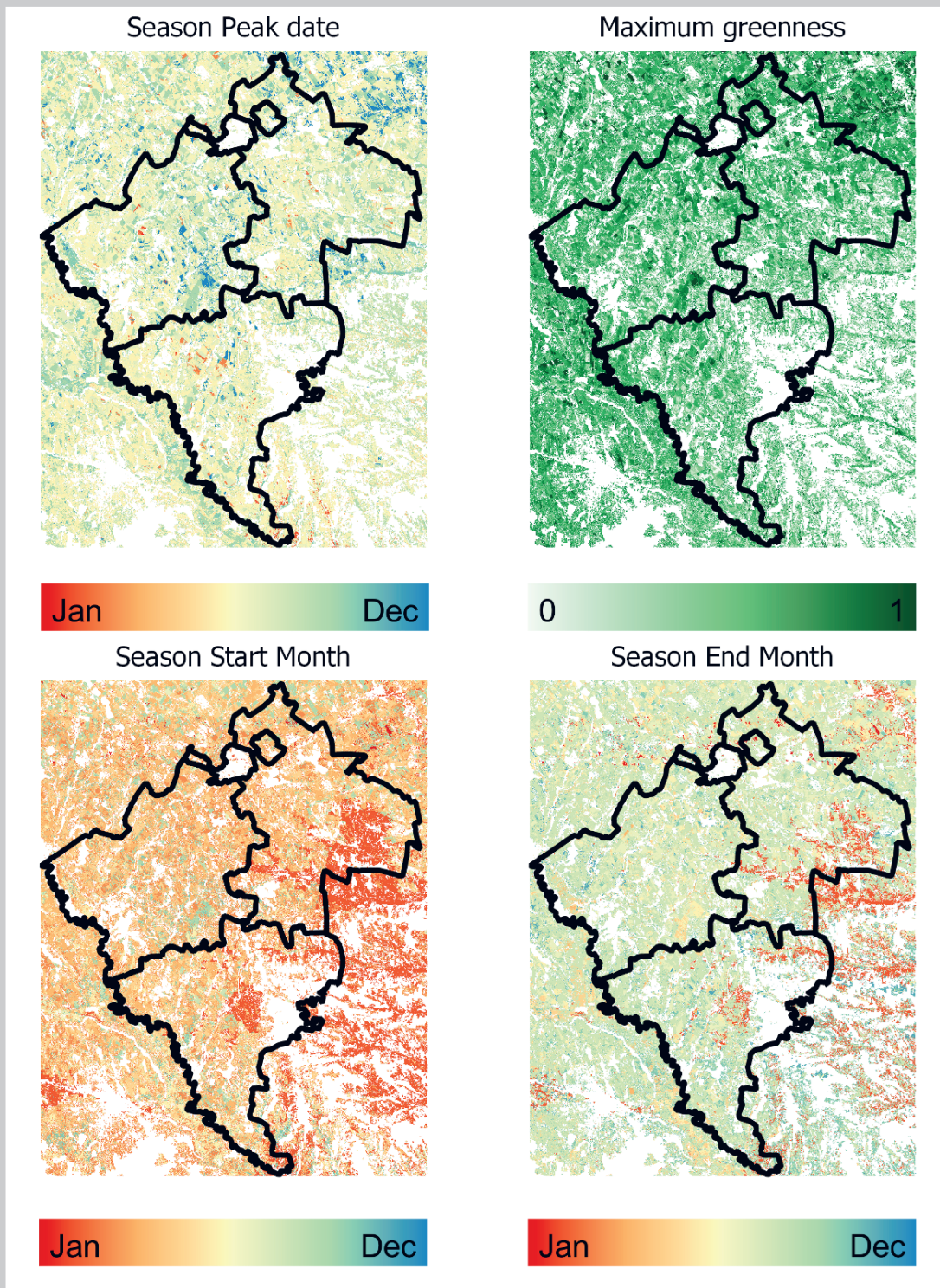
Over arable land, the **growing season** was characterized with the following raster layers:

- Season Start layer (by month)
- Season Peak layer (by date)
- Season End layer (by month)
- Maximum greenness layer (max NDVI)

in Moldova

The four layers are in raster format (Figure 3)

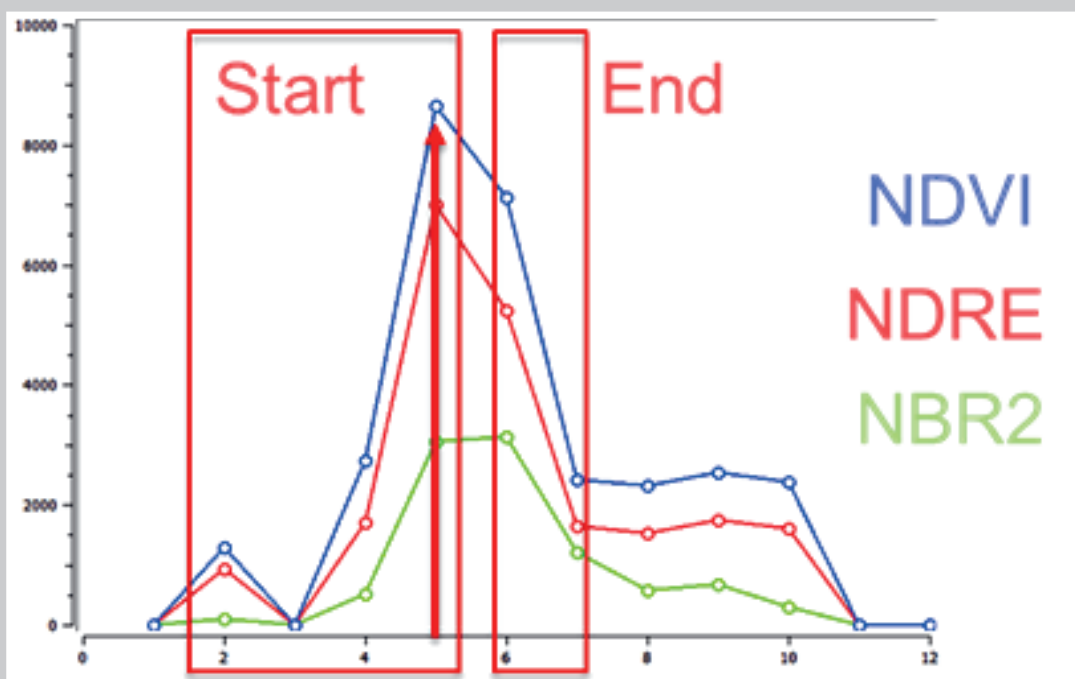
Figure 3: Season Start, Peak, End and maximum Greenness for the 2018 over the AOI.



Start and End season are derived based on the shape and gradient of different vegetation indices time series. Season start is computed as the month of maximum curvature

and positive gradient using a centred estimation of 3-points polynomial 1st and 2nd derivatives. Season end is computed as minimum gradient using a forward estimation of a 2-points polynomial 1st and 2nd derivative. Season Peak and Maximum Greenness are the acquisition date and value of the maximum NDVI, respectively (Figure 4).

Figure 4: Outline of season characterization method for Season Start Peak and End.



### Anomaly detected in 2020

For 2020, the analysis covers the period 1 January to 30 June 2020. Additionally to the output presented for the period 2017 -2019, the current season layers were aggregated at *raion* scale to highlight temporal trends and differences compared to the previous years.

Because of the limited temporal interval, data over the full growing season were not available and, as a result, the quality control checks (temporal consistency, harvesting evidence) are not completely reliable and the end of Season layer is not available.

Season Peak and Maximum Greenness layers can show the temporal differences between the years considered. However, the time series does not include data past the end of July, so it is possible that in certain areas season peaks in the months of July or August.

From the Season Peak date, little difference is noticeable between the period 2017 - 2019 and the 2020 however considering the maximum greenness it is clear a reduction of the maximum NDVI recorded over the AOI. Another important feature is the area considered as non vegetated. From Figure 5 and 6 it is clear the increment of non vegetated area.

Seasonal variation in season peak and maximum greenness can be responsible for the lower amount of vegetated areas, however, the atmospheric data recorded at the Falesti meteorological station do not show significant differences between the monthly average temperature of 2020 with respect to 2017 - 2019 (Figure 7)

Figure 5: Season Peak comparison from year 2017 (top left) to 2020 (bottom right).

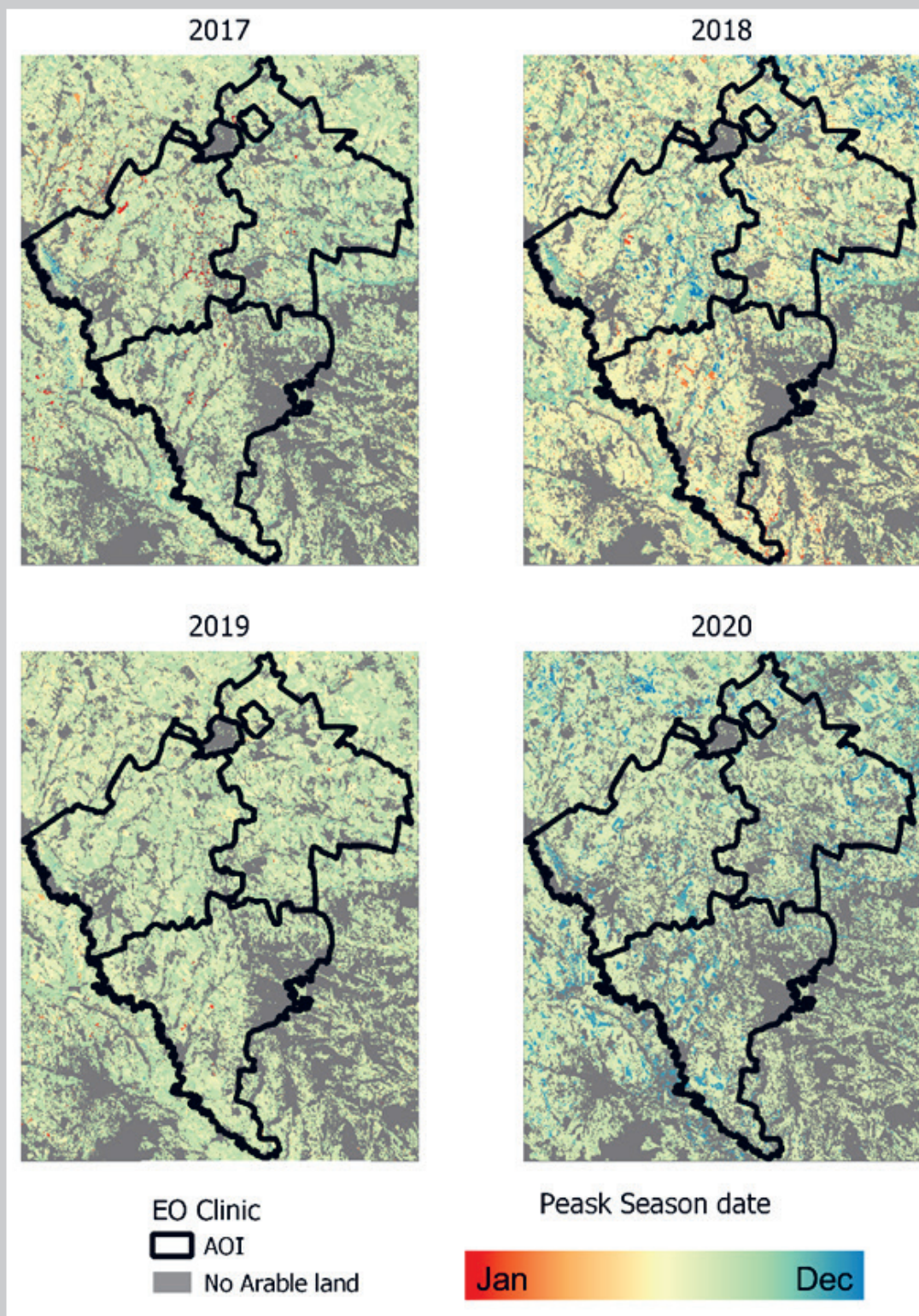


Figure 6: Maximum Greenness comparison from year 2017 (top left) to 2020 (bottom right).

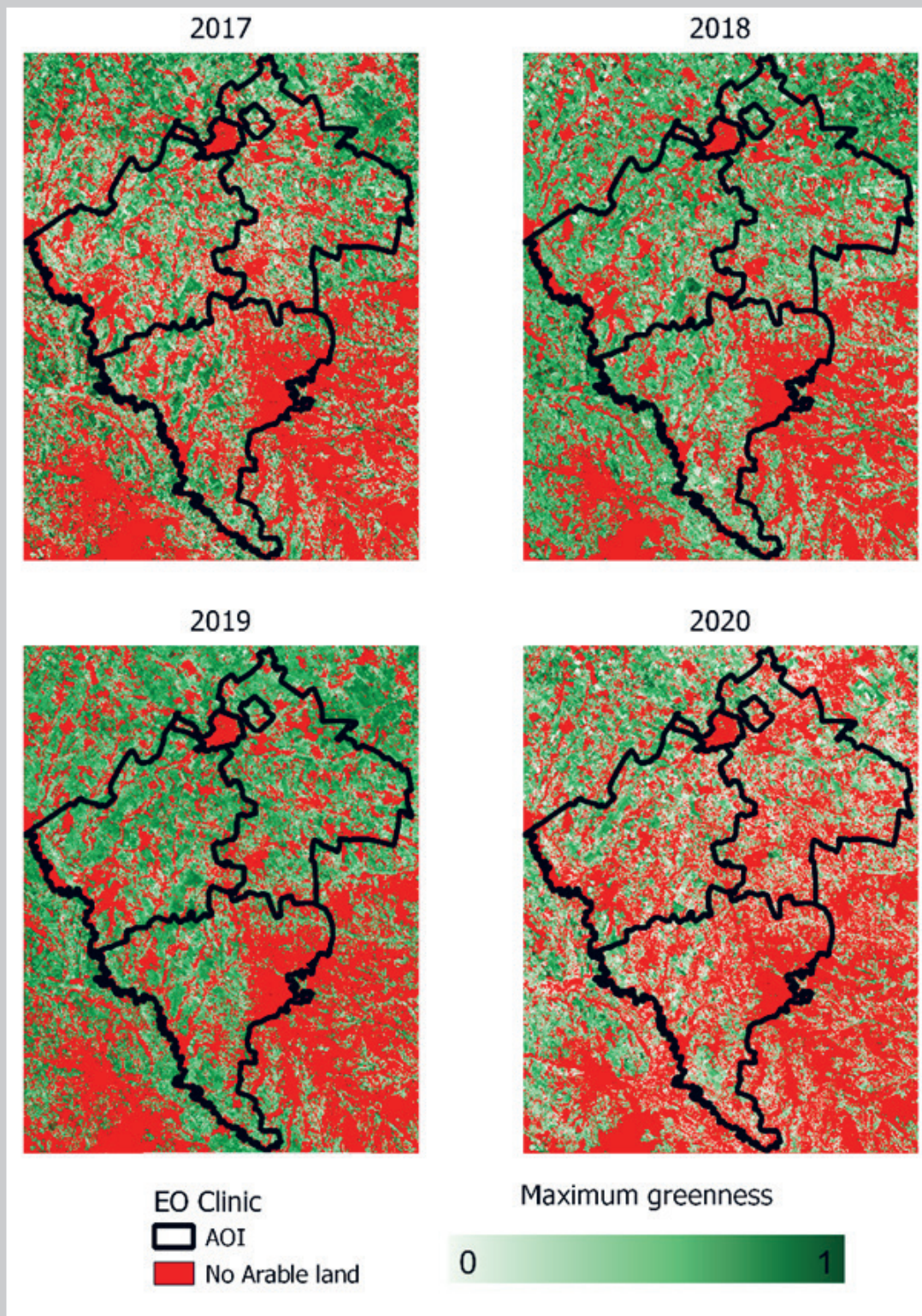
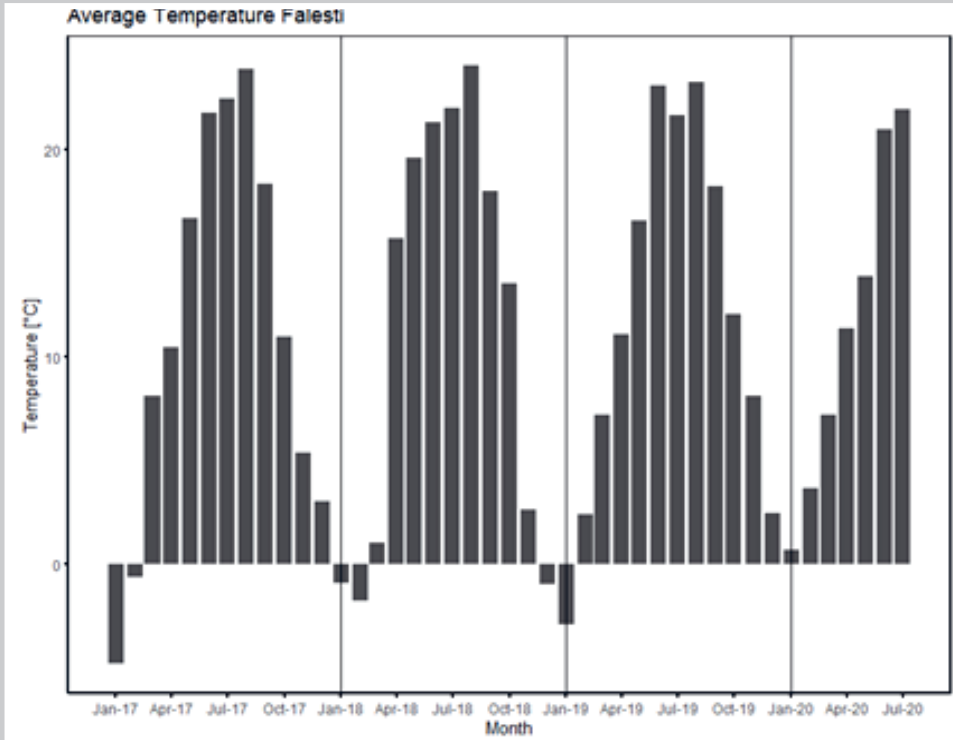


Figure 7: Average monthly time series over the station of Falesti (data is provided by the website "Reliable Prognosis", rp5.ru, and made available by the Moldova UNDP representative).



These results can also be visualized in graphs aggregated at *raion* scales. Figure 8 shows the maximum greenness for each year considered aggregated at Raion scales.

The maximum greenness level exhibit a sharp decrease for 2020, the graph does not account for differences in crop area therefore pixels identified as arable land are considerably late compared to previous years or unhealthy. Caution is advised regarding these results as it is possible that 2020 will be characterized by a late peak season in July or August.

Figure 8: Average maximum greenness for each Raion.

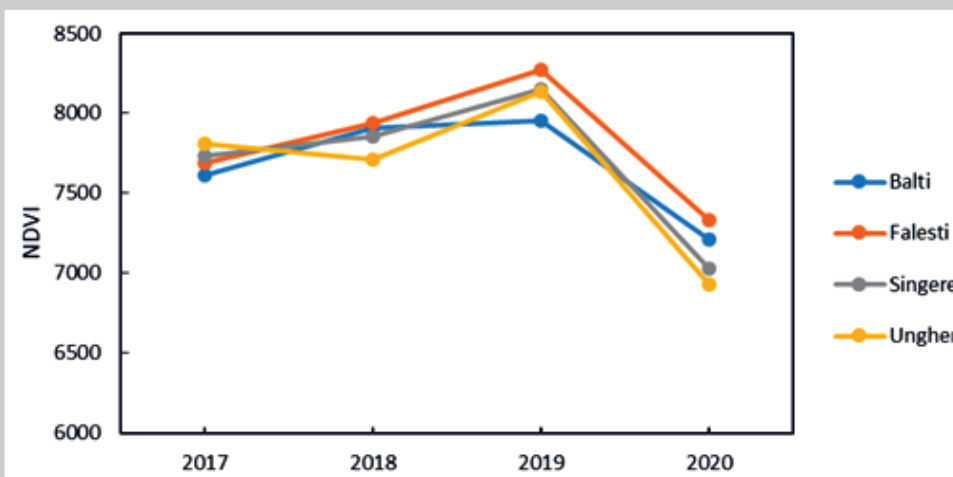
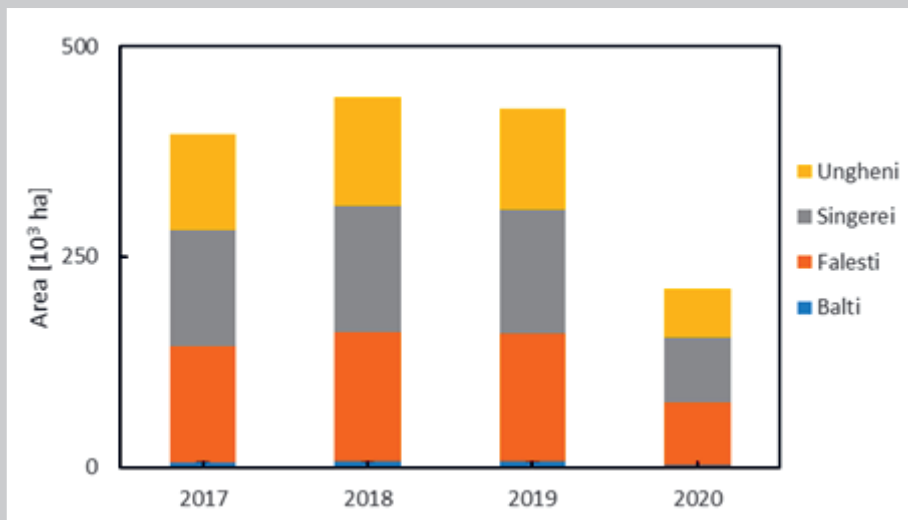


Figure 9: Total arable land for each Raion.



### 3.1.2 Quality Control and Validation

Service 1 quality checks were performed to verify the temporal consistency of results. Highest confidence values were assigned to those pixels having a consistent sequence of start of growing season, peak season, end of growing season.

The **arable crop mask** will have 3 different values in decreasing order of confidence (Figure 2):

- 1: Highest Confidence Value – Consistent temporal check
- 2: Medium Value – Possible double crop / missing data
- 4-6: Low Confidence Crop detected

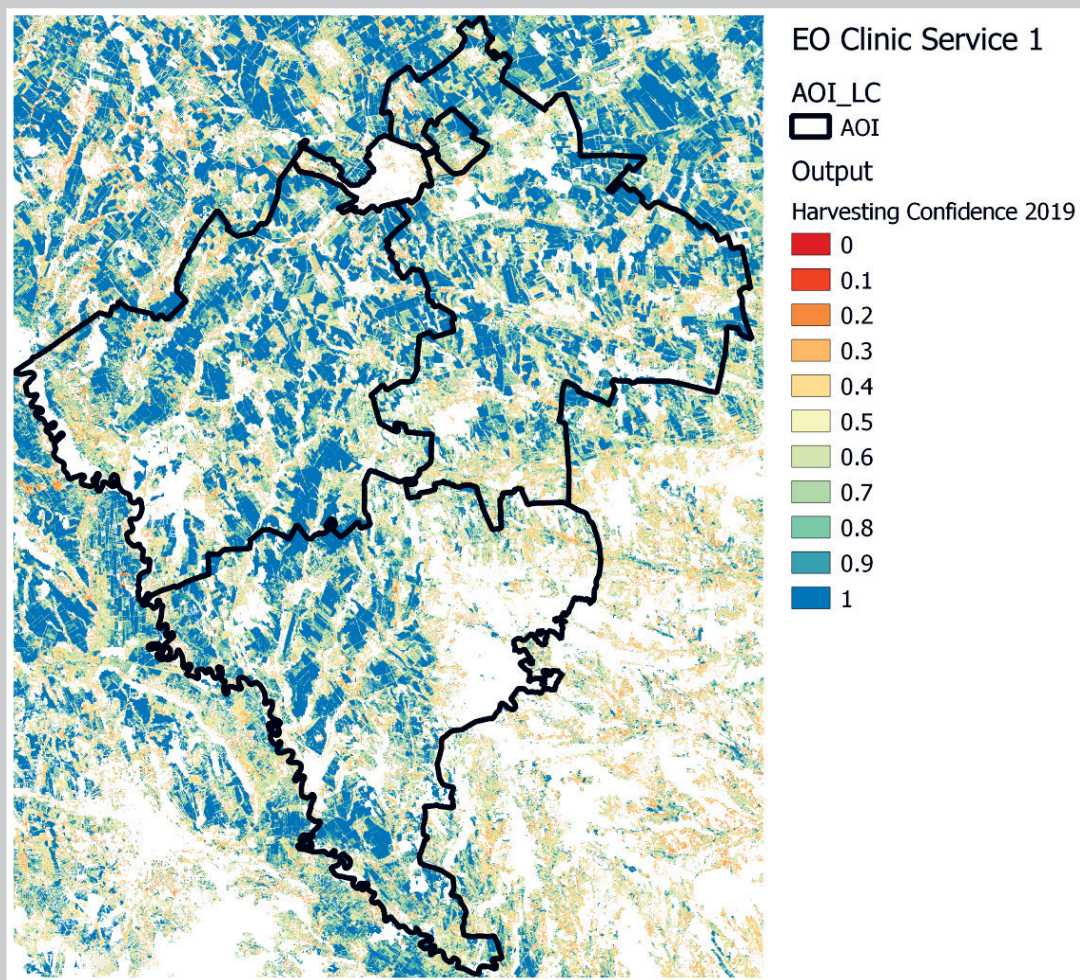
Further quality checks were performed to detect pixels showing uncertain harvesting evidence.

The harvesting confidence layer will have increasing confidence values from 0 to 1 (Figure 10).

Using this layer the output it is possible to customize the arable crop mask and exclude uncertain pixels based on the customer needs.

No validation was possible for service 1 products as not reference data was provided.

Figure 10: Harvesting Evidence confidence for the 2018 over the AOI.



### 3.1.3 Usage, Limitations and Constraints

Service 1 output products do not use training reference data, supervised classification techniques were not used and time series analysis was adopted. For this reason quality checks were introduced to verify temporal consistency of growing season and confidence in the harvesting events, which is a characteristic cereals farming practice.

Snow and cloud cover limits the number of available observation over an area. Persistent cloud cover in the first months of the year has a direct impact on the season start estimates. It is assumed that at least 1 observation is available in 5 different months of the year. Additionally, cloud, shadow and snow pixels can be included in the analysis if the Sentinel 2 product does not correctly flags them.

## 3.2 Service 2: Mobility Trends to Reveal Agricultural Practice Anomalies

### 3.2.1 Specifications

In the following, some examples of outcomes of activities carried out in Service 2 are reported.

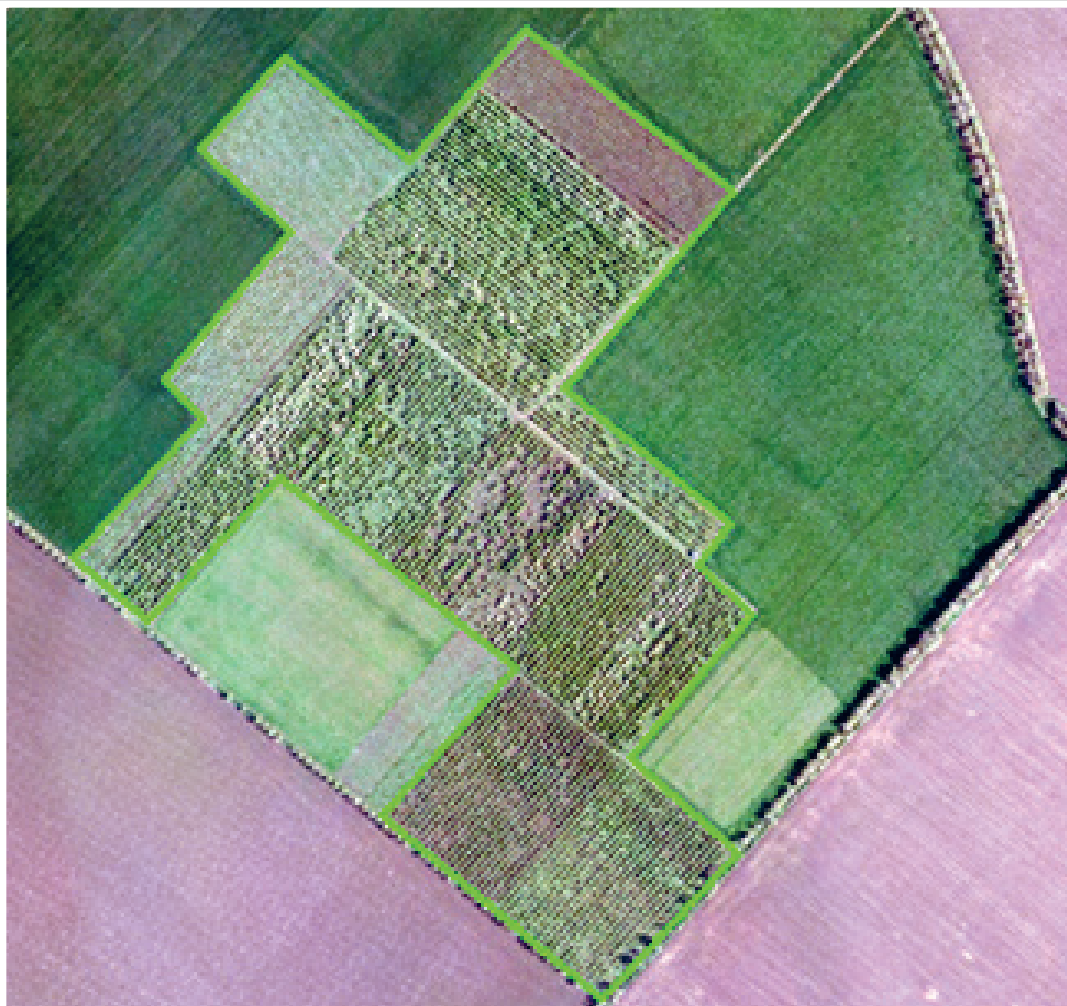
### 3.2.1.1 Analysis and evaluation of status of orchards in 2020 season

#### Mapping of orchard distribution

The first step of the Service 2 is related to orchards mapping that has been derived from 2016 orthoimagery by means of visual interpretation. The analyzed area shows a high level of fragmentation with arable land, orchard, vineyard lands and sparse natural areas.

Orchard refers to cultivated trees and/or small - medium shrubs, spatially well distributed in distinct blocks. The main recognition feature is the grid pattern based on rows of trees or bushes of equal space with a row distance of no more than 6 meters. Any single element (plant/tree crown) is well visible on the very high resolution image.

Figure 11: In the figure an example of orchard regular pattern visible on the orthophoto.



Also vineyards have been included in the orchard category, because of their role in fruit provision. Vineyards are characterized by nearby and very regular rows. The individual tree crown is not recognisable due to the intrinsic characteristics of the grapevines and the resolution of the image.

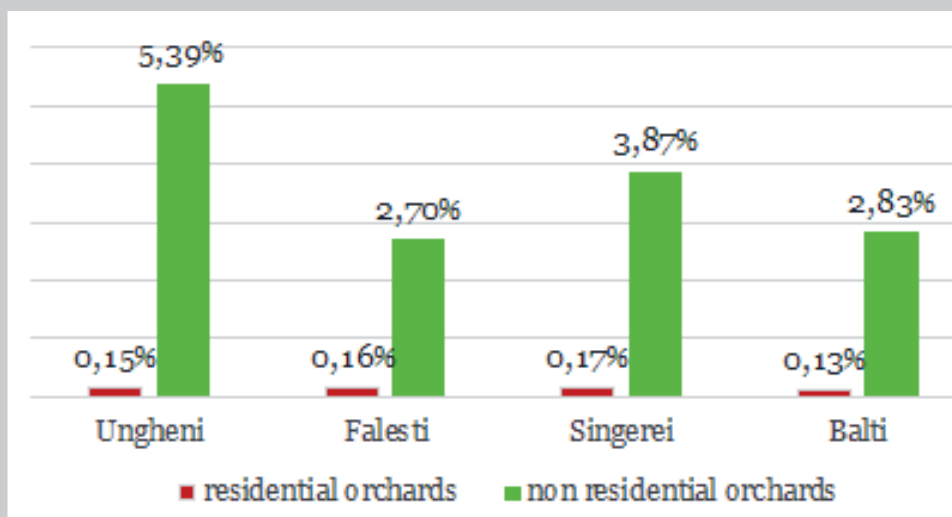
Figure 12: On the left the typical pattern of vineyard based on equally spaced rows of grapevines. On the right a photo of the identified vineyard visible on Google Earth.



In many orchards the stakes of the planting system are clearly visible<sup>6</sup> and recognizable (see TABLE 1).

The orchards have been divided into residential and non residential to facilitate later mobility analyses. Figure 13 shows the distribution of orchards divided by district and type with respect to the total area of each district.

Figure 13: Orchard distribution divided into districts.



To distinguish these two different types of orchards, two datasets have been used to uniquely identify urban areas:

- **GlobeLand30 (GL30)** (<http://www.globallandcover.com/GLC30Download/index.aspx>)

GL30 is a project of the National Geomatics Centre of China (NGCC) conducted from 2000 to 2010. The output is a global land cover dataset at 30 m spatial resolution with

an accuracy of over 80%, derived from multispectral satellite images acquired mainly from Landsat Thematic Mapper (TM), Enhanced Thematic Mapper plus (ETM+) and HJ-1 (multispectral images of Chinese Environmental Disaster Alleviation Satellite) and auxiliary data (existing regional and global land cover data, MODIS NDVI, global DEM, and free online resources). GL30 is constructed over a land use classification that consists of 10 land cover types. The entire dataset is freely available since 2014, when China donated it to the United Nations as a contribution towards global sustainable development and combating climate change.

● **OpenStreetMap (OSM) (<https://www.openstreetmap.org/>)**

OSM is one of the most prominent Volunteered Geographic Information (VGI) projects to date that implements a collaborative workflow and aims to create a freely available map database of the entire world. The OpenStreetMap Foundation is an international not-for-profit organization supporting, but not controlling, the OpenStreetMap Project. It is dedicated to encouraging the growth, development and distribution of free geospatial data and to providing geospatial data for anyone to use and share.

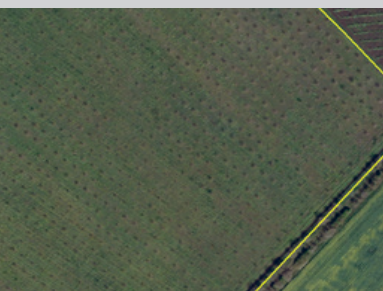
These two datasets were used together in order to have a complete urban coverage of the whole area of interest. OSM, in fact, has a higher geometric accuracy but, unfortunately, it has some missing areas; consequently, GL30 has been used in order to cover these gaps. All orchard polygons within the urban dataset are classified as residential.

The following table shows the types of orchards identified within the area of interest.

Table 1: **Types of orchards identified within the area of interest.**

Orchard type	Orchard image	Note
Orchard non residential		outside of residential areas, regular pattern, visible implant system stakes, slightly visible plant crowns
Orchard non residential		outside of residential areas, regular pattern, clearly visible plant crowns

in Moldova

Orchard type	Orchard image	Note
Orchard non residential		outside of residential areas, regular pattern, clearly visible plant crowns, flowering plants
Orchard non residential		outside of residential areas, regular pattern, no visible implant system stakes, square implant pattern, visible plant crowns, grassy row spacing
Orchard non residential		outside of residential areas, regular pattern, visible implant system stakes of vineyards, no visible plant crowns
Orchard non residential		outside of residential areas, regular pattern of vineyards, visible implant system stakes, visible non regular plant crowns
Orchard residential		inside of residential areas, regular pattern, clearly visible implant system stakes

High resolution satellite image on Google Earth have been used to improved and make easier the visual interpretation of the area.

Once the orchard photo-interpretation phase is finished, a visual inspection and refinement phase has been carried out to ensure the consistency and the homogeneity of the product generated by each interpreter. Finally, a quantitative independent validation has been conducted in order to validate the product produced (see 3.2.2).

Figure 14: **Example of spatial distribution of orchards in Falesti district. Orchards have been distinguished between residential and not residential. Residential orchards are localised within or closed to urban areas.**



Main limitations encountered during the visual interpretation have been:

- the acquisition period, in the year, of available high resolution imagery, as some orchards are not well recognizable at the beginning of the growing season (*supposed acquisition period*);
- the presence of tree plantation and reforestation areas whose regular pattern is often confusing with orchard one.

### **Vegetation characterization and mapping of 2020 vegetation status in AOI**

Sentinel-2 NDVI time-series have been generated for the whole AOI, and NDVI function modelling and phenological parameters extraction and analysis have been performed for 2017, 2018, 2019 and 2020 years. A preliminary phase, aimed at defining and testing different parameter configurations to be used for NDVI time-series modelling purposes to be subsequently adopted for the analysis of the whole AOI, has been carried out taking into consideration two different test areas (Figure14).

In the following Figure 15, FIGURE 1716 and FIGURE 17 are some examples of maps showing the spatial distribution at pixel level of phenological parameters obtained for the 2019 vegetation growing season. Similar maps, summarizing phenological parameters for each

in Moldova

growing season occurred in the interval 2017-2020, and covering the whole AOI, have been produced. The information contained in these maps can be considered as base data in order to generate derived value-added information. Main statistical metrics for each examined phenological parameter have been also evaluated at orchard level considering all the pixels belonging to each orchard polygon (see FIGURE 9 and 20) in order to support the orchard characterization in the examined AOI. The investigation of the temporal dynamic of these values for the whole time-series 2017-2020 could support the identification of the key development stages for orchard areas in AOI (TABLE 2 shows an example of outcomes temporally and spatially integrated over the whole AOI, considering a simple average rule). Different rules could be selected and applied on supplied datasets, in order to derive proper aggregations and supporting different purposes.

Figure 15: **Test areas identified in the AOI in order to check the complete procedure for seasonal NDVI function fitting and phenological parameters extraction.**

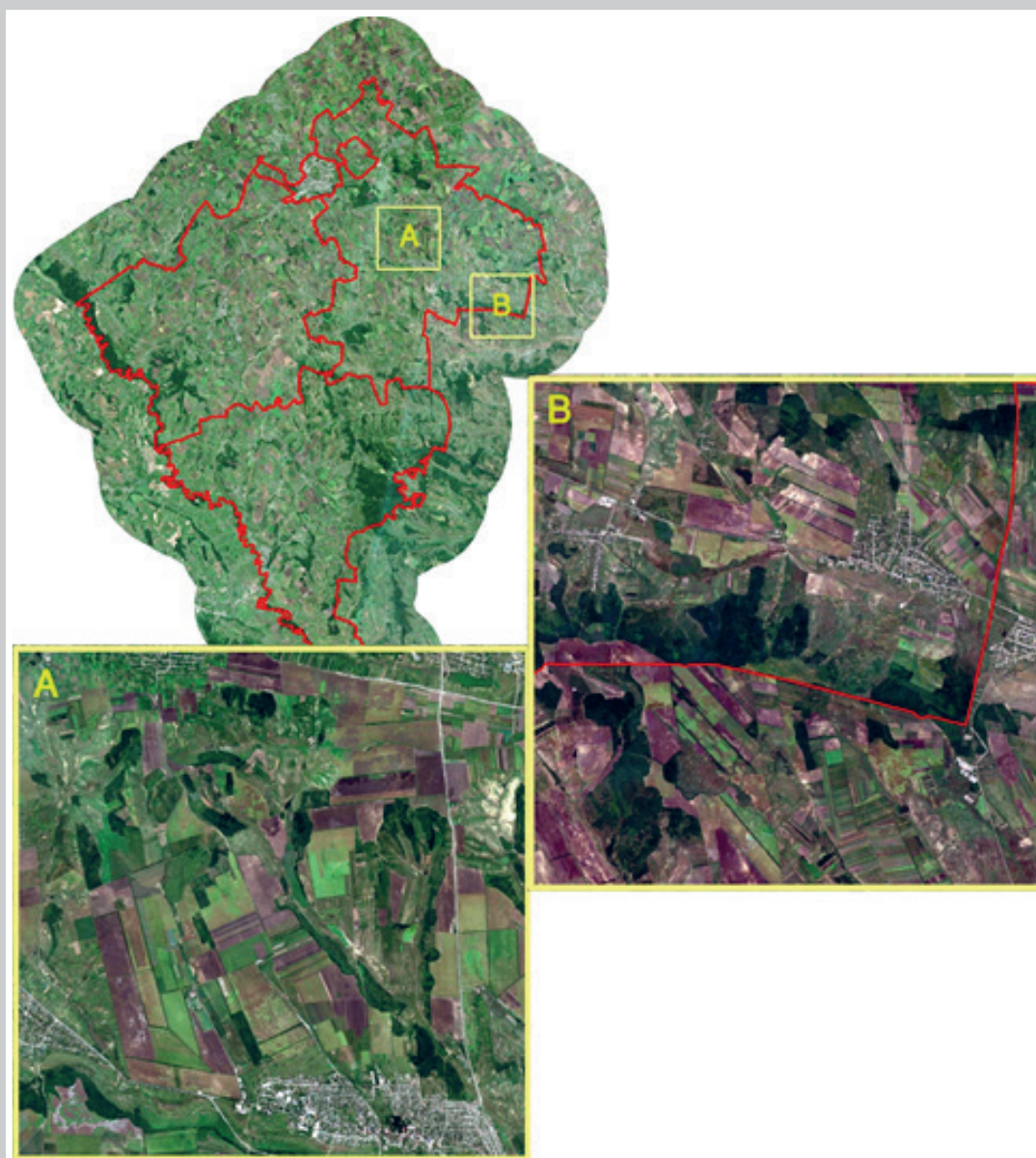


Figure 16: Examples of Start Of Season (left image) and Mid Of Season (right image) phenological parameter maps produced from Sentinel-2 NDVI time-series (pixel level, only orchard areas are represented in map) for the 2019 vegetation growing season.

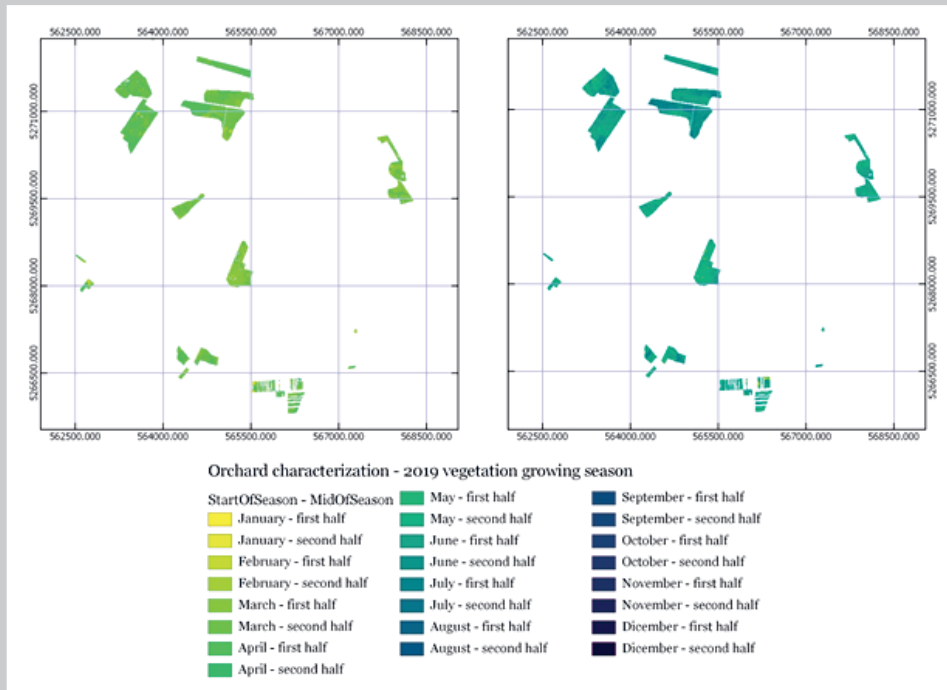


Figure 17: Examples of maps of seasonal Amplitude (right image) and Length (left image) phenological parameters produced from Sentinel-2 NDVI time-series (pixel level, only orchard areas are represented in map) for the 2019 vegetation growing season.

According to obtained outcomes, orchard areas and natural vegetated areas generally show longer seasonal photosynthetic activity (high seasonal length values, generally 6-9 months) respect to crop areas. The analysis of the Amplitude parameter helps to identify the areas where high dynamics in the NDVI values are observed in the examined growing season. In this case, this parameter shows comparable values for orchard and crop areas.

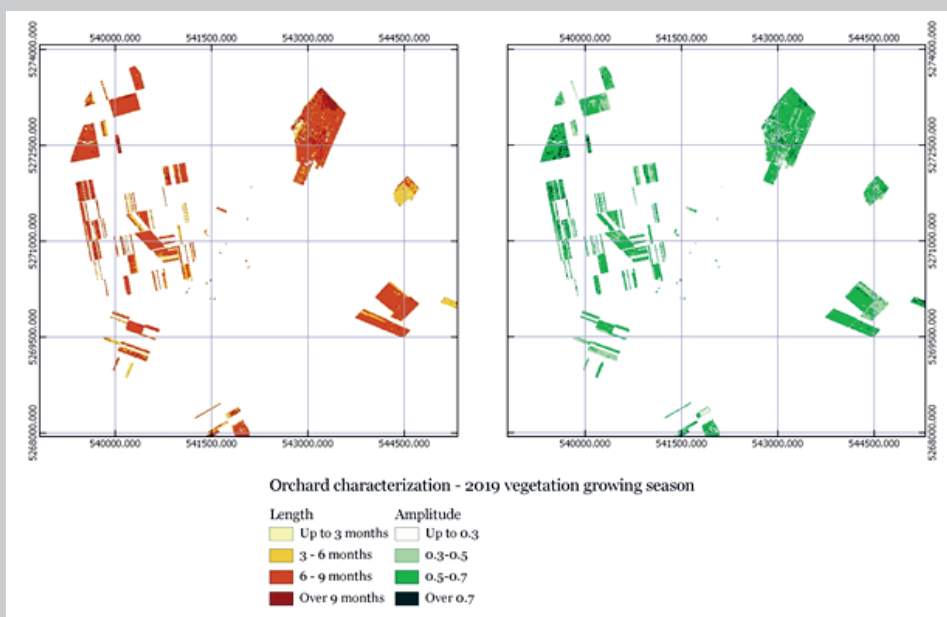


Figure 18: Examples of statistical metrics evaluated at orchard level for each growing season in the time-series 2017-2020 and for all the examined phenological parameters. In the example in figure, statistical metrics refer only to the Start of Season and Seasonal Small Integral parameters evaluated in the 2019 growing season and to the orchard polygon highlighted in yellow circle.

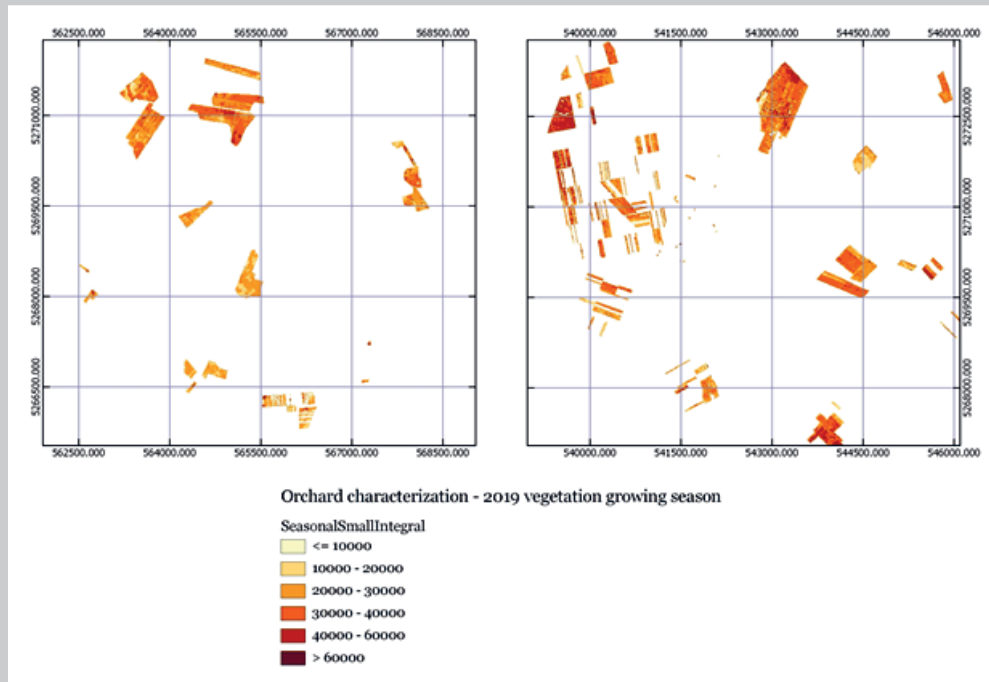


Figure 19: Examples of statistical metrics evaluated at orchard level for each growing season in the time-series 2017-2020 and for all the examined phenological parameters. In the example in figure, statistical metrics refer only to the Start of Season and Seasonal Small Integral parameters evaluated in the 2019 growing season and to the orchard polygon highlighted in yellow circle.

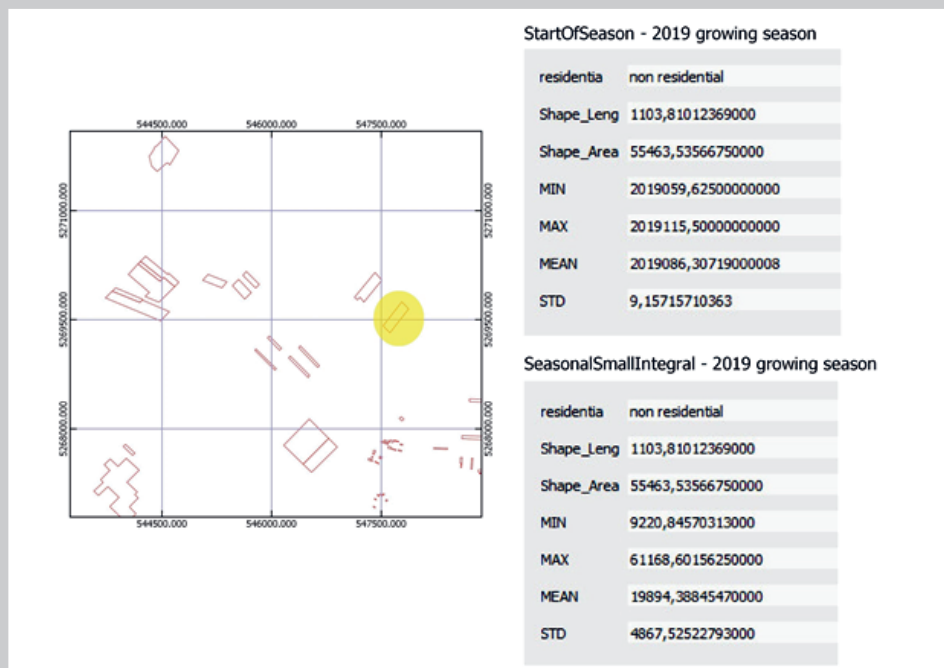


Figure 20: Example of map of the Seasonal Small Integral (SMI) phenological parameter produced at pixel level (left image, outputs are produced in raster format) and orchard level (right image, outputs are produced as polygon vectors with statistic metrics, as in FIGURE 9) for the 2019 vegetation growing season.

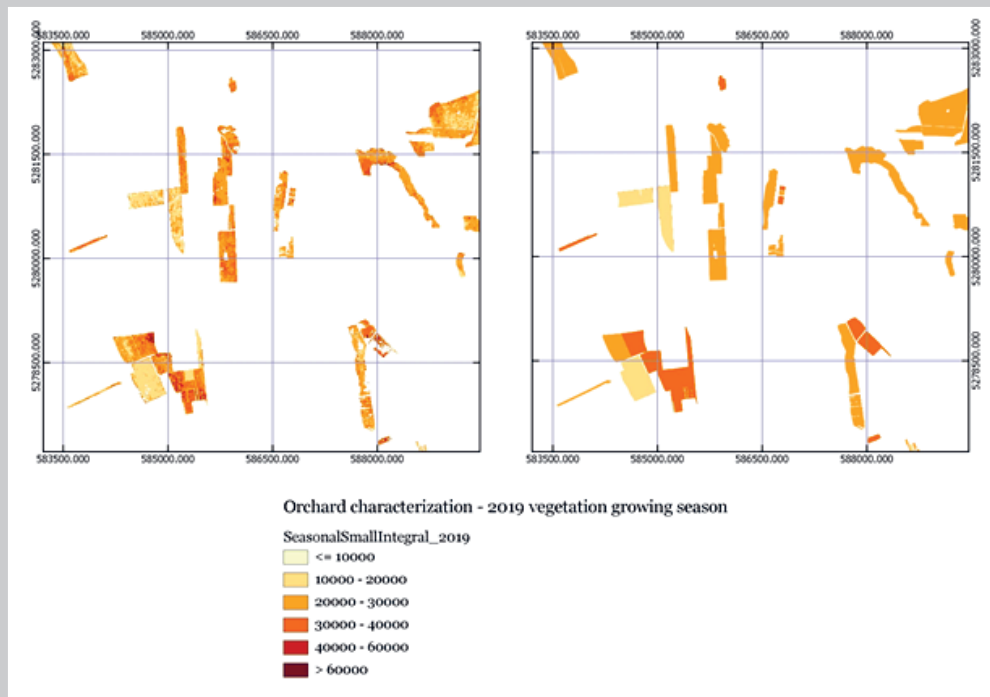


Table 2: Table summarizing the examined phenological parameter values, temporally and spatially integrated over all the orchard polygons belonging in the AOI, according to an average rule.

<b>AMPLITUDE</b>				
	<b>min</b>	<b>max</b>	<b>mean</b>	<b>stdev</b>
<b>2017</b>	3440,7	9935,9	5792,8	1407,6
<b>2018</b>	3343,2	8985,3	5321,4	1218,2
<b>2019</b>	3741,6	7045,2	5130,7	633,4
<b>mean 2017-2019</b>	3508,52	8655,46	5414,94	1086,4
<b>2020</b>	3579,4	6228,1	4796,9	817,9
<b>LENGTH [months]</b>				
	<b>min</b>	<b>max</b>	<b>mean</b>	<b>stdev</b>
<b>2017</b>	4,7	10,8	7,5	1,4
<b>2018</b>	5,7	10,1	7,9	0,9
<b>2019</b>	1,1	20,9	6,7	0,8
<b>mean 2017-2019</b>	3,9	13,9	7,4	1,1
<b>2020</b>	5,6	10,0	7,8	0,9

<b>MID [DOY]</b>				
	<b>min</b>	<b>max</b>	<b>mean</b>	<b>stdev</b>
<b>2017</b>	141	238	188	19
<b>2018</b>	137	225	183	16
<b>2019</b>	141	200	173	11
<b>mean 2017-2019</b>	140	221	181	15
<b>2020</b>	159	240	194	15
<b>SMI</b>				
	<b>min</b>	<b>max</b>	<b>mean</b>	<b>stdev</b>
<b>2017</b>	14911,0	80134,8	34660,9	14234,9
<b>2018</b>	16550,5	66652,9	32388,1	10729,3
<b>2019</b>	15522,3	43842,6	25343,9	5225,2
<b>mean 2017-2019</b>	15661,3	63543,4	30797,7	10063,1
<b>2020</b>	14527,5	58086,7	29611,2	9886,7
<b>SOS [DOY]</b>				
	<b>min</b>	<b>max</b>	<b>mean</b>	<b>stdev</b>
<b>2017</b>	42	155	86	19
<b>2018</b>	35	137	77	16
<b>2019</b>	59	117	89	11
<b>mean 2017-2019</b>	45	136	84	15
<b>2020</b>	53	146	90	15

Following Figure 21 shows some examples of maps of deviations in the Start of the Season and Small Integral phenological parameters, evaluated at pixel level for the 2020 vegetation growing season respect to the average values obtained from the reference time-series 2017-2019. Negative deviations observed in the Small Integral parameter may help to identify orchard areas where reduction in vegetation greenness and biomass are expected for the 2020 growing season respect to previous years, according to the NDVI temporal evolution modelled starting from available satellite imagery (up to May 2020). Moreover, the deviations in the Start of the Season parameter have to be interpreted in terms of possible advances or delays in the start of the photosynthetic activity (as registered in satellite observations and modelled using proposed methodology) for the 2020 growing season respect to previous years. As visible in the figure, two different classification schemas have been selected in order to help the interpretation of observed deviations. Moreover, the outcomes of deviation analysis have been also evaluated and mapped at orchard field level using the same classification schemas. For this purpose, each orchard polygon in the examined AOI has been assigned to a particular deviation class and type according to a frequency rule applied considering the deviations classes/types of all the pixels that belong to it. See examples in Figure 21 and Figure 22. These maps support the identification of priority areas for subsequent analysis, described in 3.2.2.2, helping also the proper interpretation of obtained results and models in these areas.

Figure 21: Examples of maps showing the spatial distribution of the Start of Season shifts (on the left) and of the percent deviations of the Seasonal Small Integral parameter (on the right) for the 2020 vegetation growing season respect to reference average values observed in 2017-2019 seasons, evaluated at pixel level (outputs are supplied in raster format).

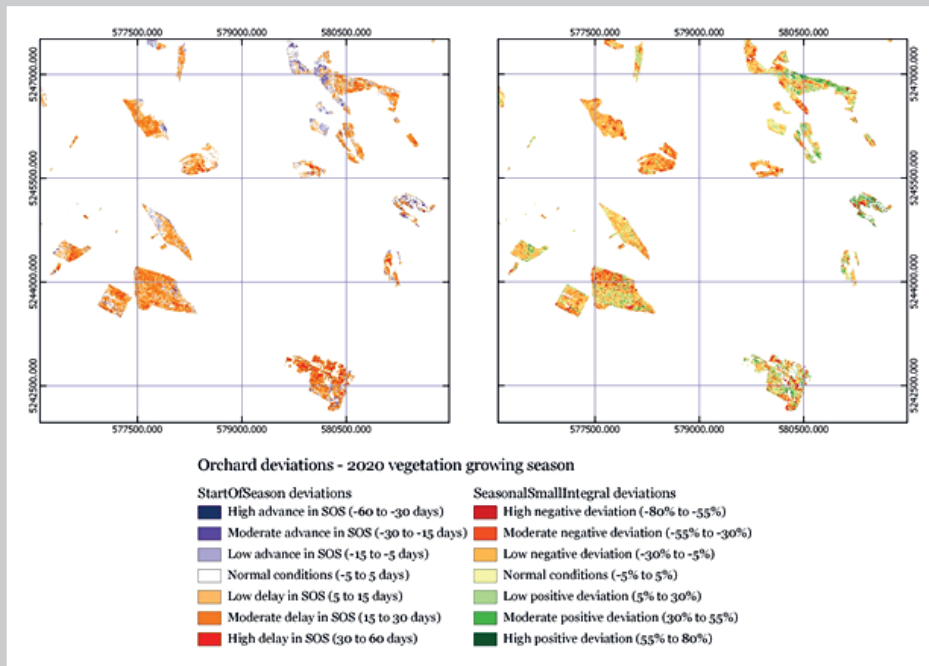


Figure 22: Example of classification at orchard level for 2020 Seasonal Small Integral parameter deviations.

For each orchard polygon in the AOI, the frequencies registered for all the deviations classes of the same typology (negative, positive or normal conditions), evaluated at pixel level, are added in order to assign the final deviation type to the polygon, considering a maximum frequency rule. Subsequently, to each orchard polygon showing a specific deviation type, the particular deviation class is assigned, according to the selected classification schema, considering the deviation class evaluated at pixel level, in the deviation type, which shows the maximum frequency in the polygon. Deviation class, for each polygon, is reported in the “anomaly\_cl” field in the table, while the general deviation type is reported in the “anomaly\_ty” field (see example of attributes reported for the orchard polygon in the yellow circle; domains of “anomaly\_cl” and “anomaly\_ty” fields are also shown).

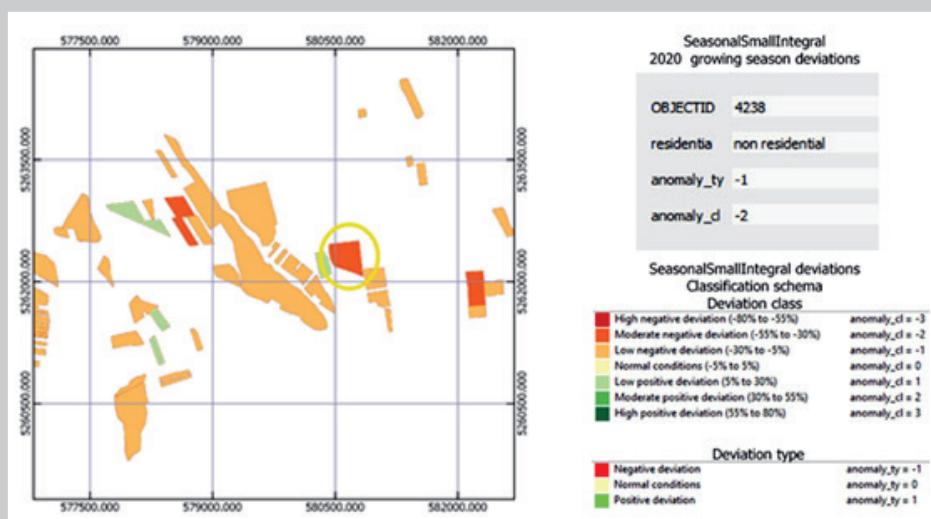
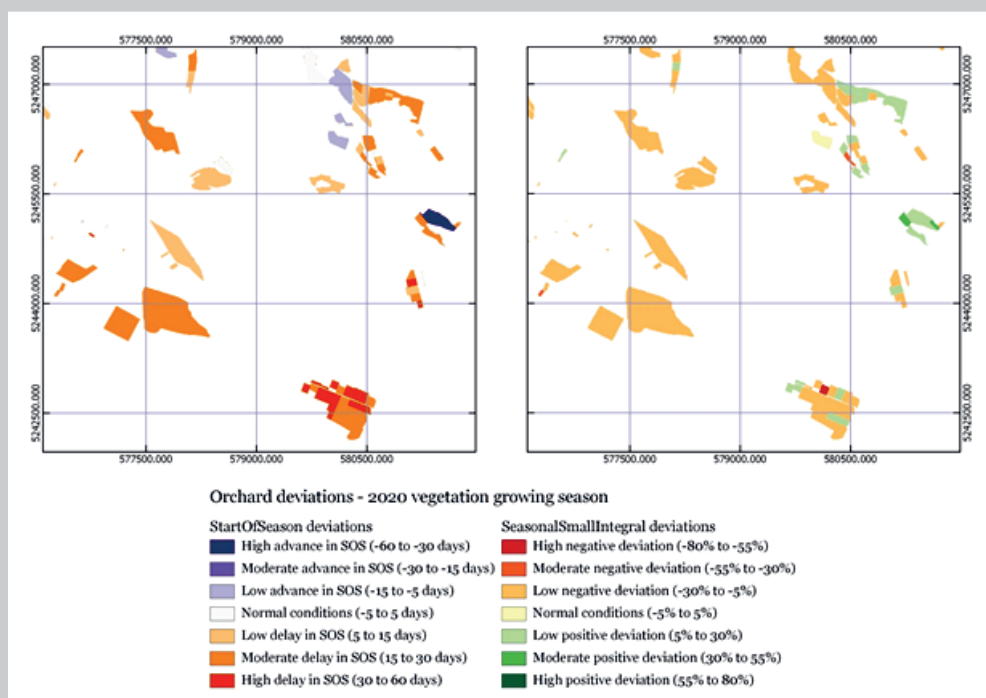


Figure 23: Examples of maps (see, for comparison, Figure 22) showing the classes of deviation for the Start Of Season shifts (on the left) and of the percent deviations of the Seasonal Small Integral parameter (on the right) parameters evaluated for the 2020 growing season respect to reference average values observed in 2017-2019 seasons, produced at orchard level (outputs are polygon vectors with classification details, as in Figure 24).



Following TABLE 3, summarizes the outcomes of deviation analysis, evaluated and mapped at orchard field level, over the whole AOI. As it can be observed, the majority of orchard fields in the AOI, show low delays in the Start of the Season parameter, and low negative deviations in the Seasonal Small Integral parameter.

Table 3: Distribution in the whole AOI of the deviations of Seasonal Small Integral and Start Season phenological parameters for the 2020 growing season respect to average values (2017-2019), evaluated at orchard field level.

Start Of Season shifts			
	Residential orchard	Not residential orchard	
High advance (-60 to -30 days)	66	136	951
Moderate advance (-30 to -15 days)	99	188	
Low advance (-15 to -5 days)	121	341	
Normal conditions (-5 to 5 days)	223	360	583
Low delay (5 to 15 days)	577	1596	4153
Moderate delay (15 to 30 days)	395	1221	
High delay (30 to 60 days)	97	267	
<b>Total</b>	<b>1578</b>	<b>4109</b>	
Seasonal Small Integral percent deviations			
	Residential orchard	Not residential orchard	
High negative deviation (-80% to -55%)	55	81	4624
Moderate negative deviation (-55% to -30%)	435	751	
Low negative deviation (-30% to -5%)	816	2486	
Normal conditions (-5% to 5%)	62	60	122
Low positive deviation (5% to 30%)	149	475	941
Moderate positive deviation (30% to 55%)	52	191	
High positive deviation (55% to 80%)	9	65	
<b>Total</b>	<b>1578</b>	<b>4109</b>	

**3.2.2.2 Detection of possible Covid-19 hotspots and their correlation with vegetation status**

The four administrative areas which compose the Area of Interest are quite differentiated: Balti is a municipal administrative level, and the other ones are rayons. Balti is characterised by urban areas (over 55% of the extent), as can be view also by the composition of population, which is urban for over 90%. The other rayons (Falesti Singerei, Ungheni) are more characterised by rural areas (over 65% of the land in average), as can be noted also by the high rates of rural population, which are over 60% of total population. TABLE 4 reports some information about the extent of crops and orchards areas (as defined in 2.2 chapter). In Figure 24, the population density in 2019, with the distribution of population in 2019 between rural and urban and between working and not working age, is shown. In particular, the distribution of population by working age population seems comparable over the Area of Interest.

Figure 24: Density population in 2019 in the area of interest. Added pie charts show the distribution of the population in rural and urban (left), and under, in and over working age (right).

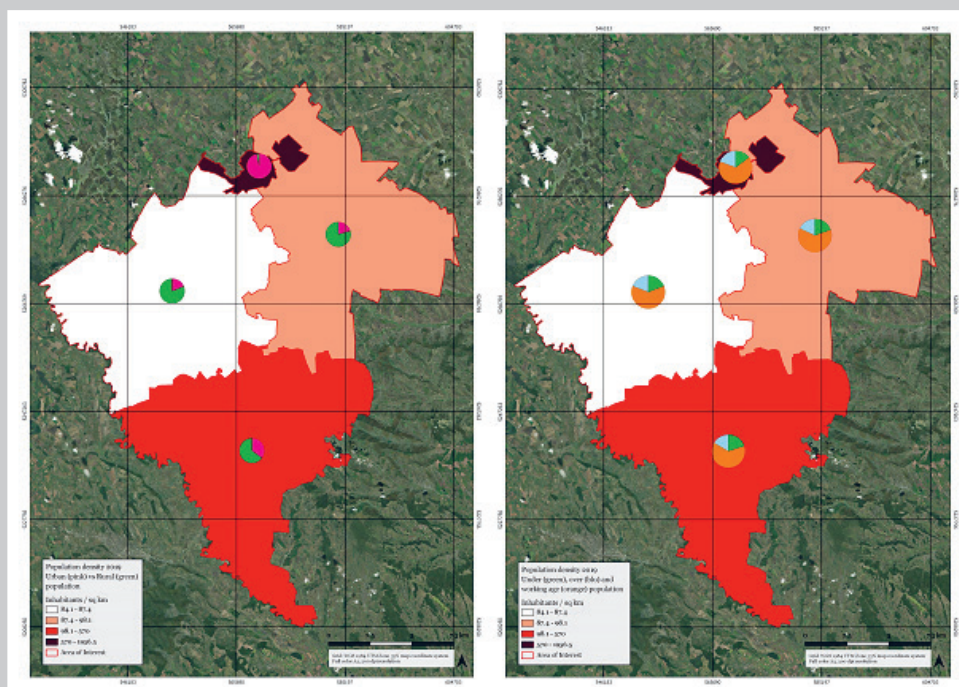


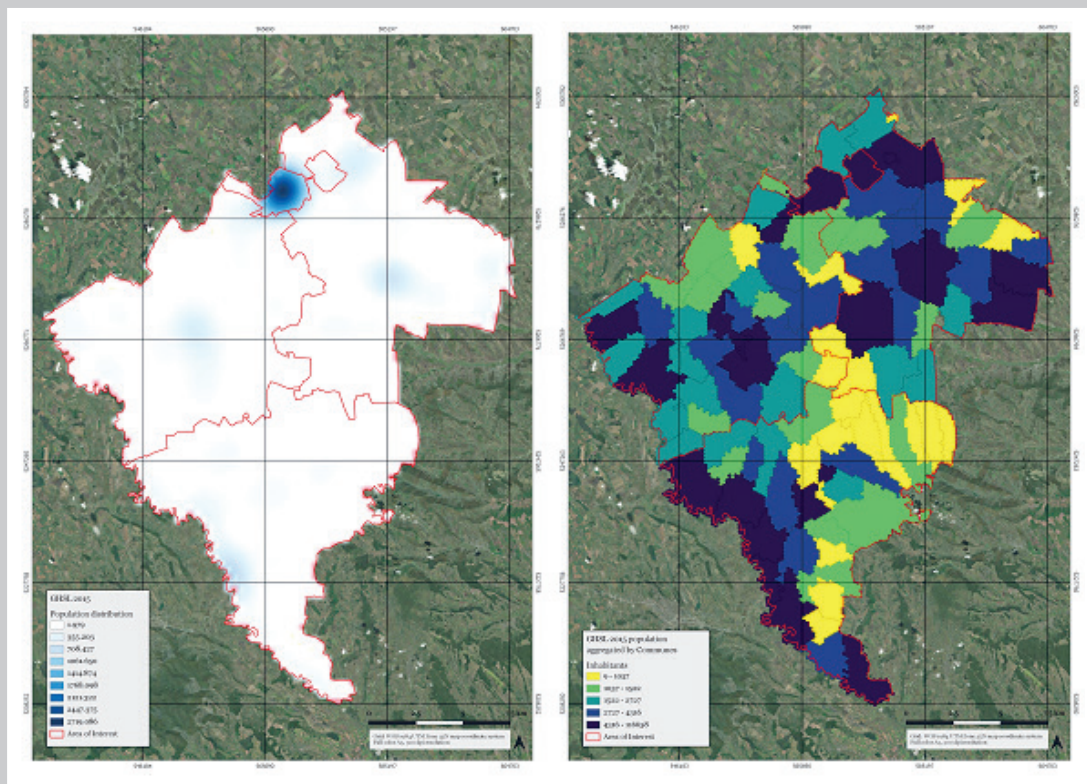
Table 4: Distribution of agricultural areas by rayon.

Admin. division	Area (km <sup>2</sup> )	Crop	Orchard	% Crops	% Orchards	% Agricultural area
Balti	77.53	32.50	2.19	41.92%	2.82%	44.74%
Falesti	1072.23	740.44	29.30	69.06%	2.73%	71.79%
Singerei	1032.95	710.24	40.18	68.76%	3.89%	72.65%
Ungheni	1081.66	571.16	59.46	52.80%	5.50%	58.30%
<b>Total AOI</b>	<b>3264.37</b>	<b>2054.35</b>	<b>131.13</b>	<b>62.93%</b>	<b>4.02%</b>	<b>66.95%</b>

in Moldova

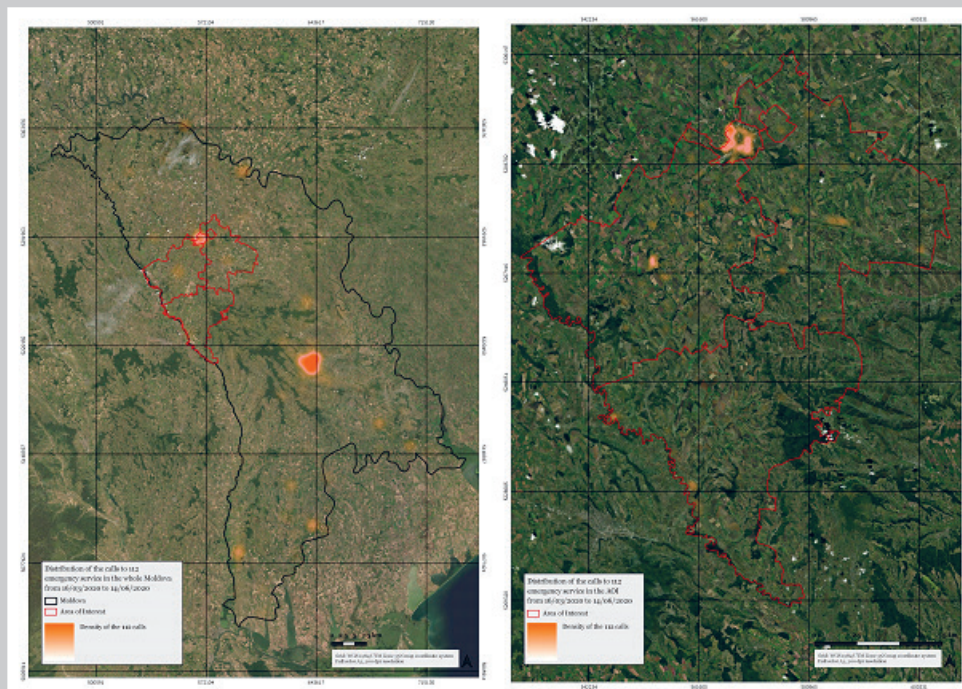
The population distribution in the area has also been analysed for the 2015 Global Land Settlement Layer source. In Figure 25 the spatial distribution of the population is shown on the left, and the population of GHSL aggregated by Municipalities boundaries (extracted through the hexagonal grid as described in 2.2 chapter) is depicted on the right. The finer spatial granularity available for the GHSL data respect to the data from Moldova Statistic portal has been considered decisive in order to better represent the population distribution in the area.

Figure 25: Density population for 2015 in the area of interest, derived by GHSL data is shown on the left. The right image shows the GHSL population aggregated by municipalities.



The distribution of the 112-emergency call (in absolute number) for Covid-19 suspicious cases seems to reflect the Covid-19 cases distribution: relevant number of 112 calls are located only in urban areas. In Figure 26, a density map shows the total number of calls in the time window available (from 16/03/2020 to 14/06/2020).

Figure 26: Heatmap representing the distribution of the 112-emergency service call, registered as suspicious cases of covid-19. Left figure shows the Moldova situation. The situation in the AOI is shown on the right.



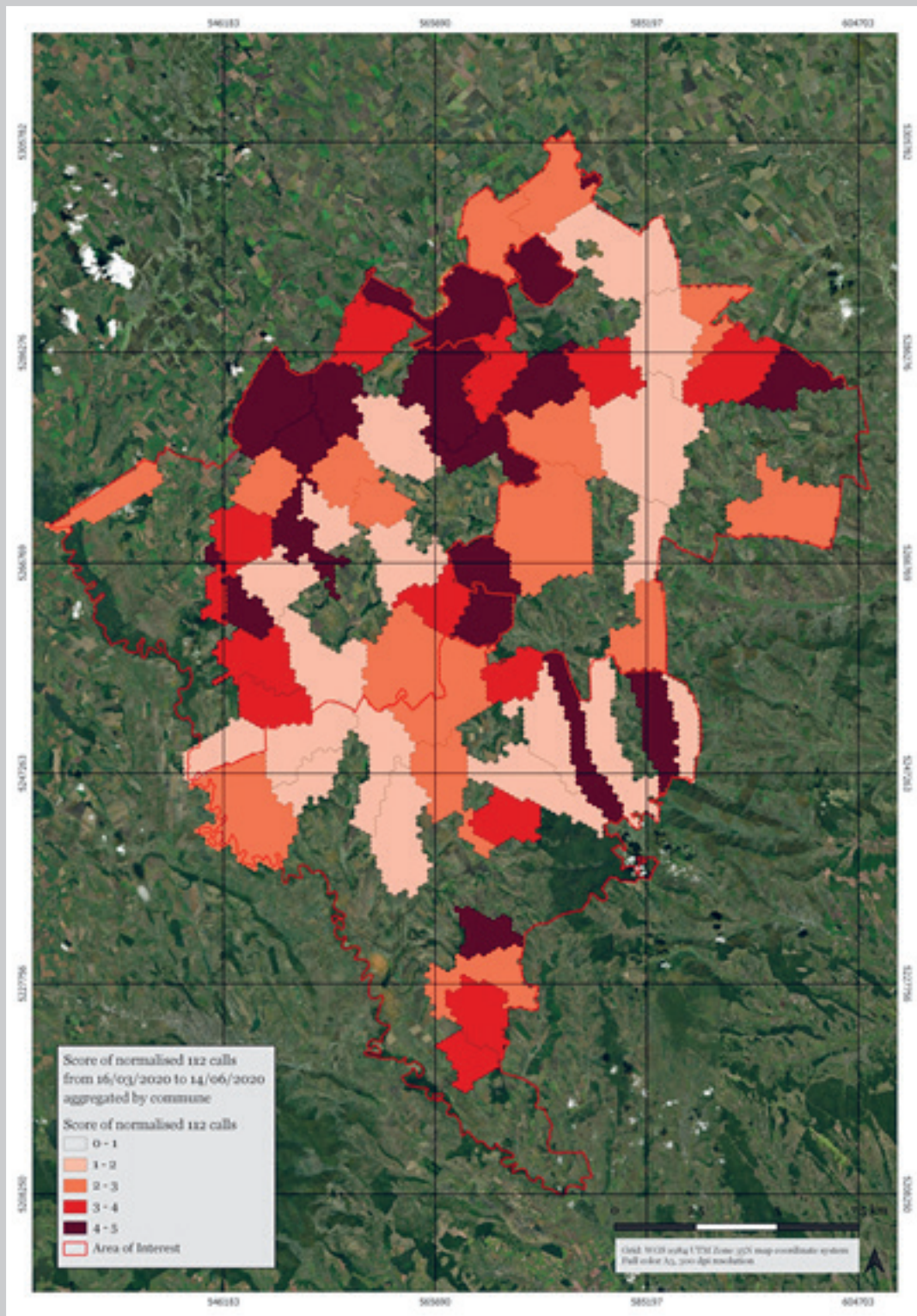
The further step was to normalise the calls data on GHSL population, the detailed procedure is described in Chap. 2.2. In TABLE 5, the values aggregated by rayons are shown; at this level also, Balti seems to be the more affected area depicts the situation of the score of the calls, at municipality level, showing a more diversified situation.

Table 5: Total calls and population in absolute numbers, average of the normalised calls on GHSL population.

Admin. Division	Total Calls	Population	Average normalised Calls on Population	Average score of Calls
Balti	960	118 057	1.09	5.00
Falesti	450	95 282	0.73	2.91
Singerei	321	90 612	0.65	2.59
Ungheni	269	110 252	0.61	2.25
<b>Total AOI</b>	<b>2 000</b>	<b>414 203</b>	<b>0.67</b>	<b>2.64</b>

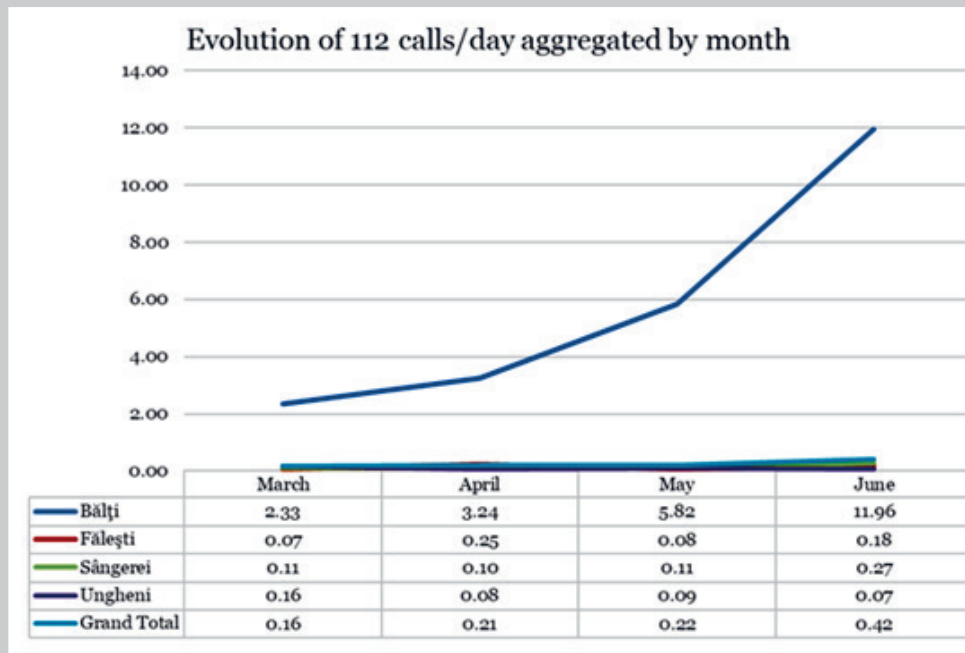
in Moldova

Figure 27: Distribution of the total calls to 112, normalised by population and classified from 1 to 5 score.



In order to assess the evolution of the 112 calls during the available temporal window, the average daily number of calls for month is shown in Figure 28. Looking at the trend, the outbreak is still in evolution as for the 14 June 2020. This evidence is also confirmed by the ESRI online dashboard platform (based on the ArcGIS COVID-19 of John Hopkins), which shows the trend of the new cases of Covid-19 in Moldova.

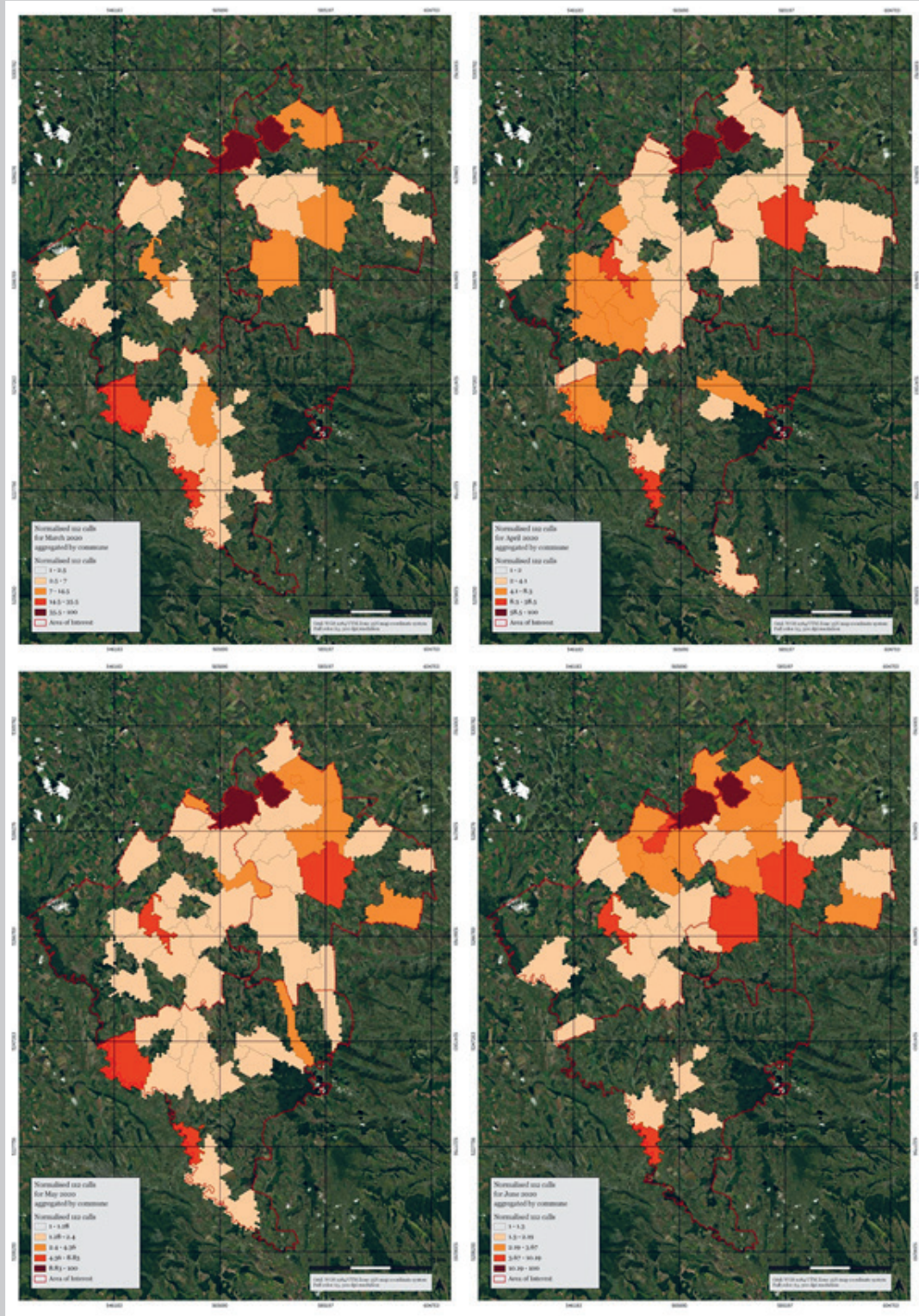
Figure 28: Trend of the 112 emergency calls by day, aggregated by month for the rayons in the Area of Interest.



The following set of maps (Figure 29) shows the evolution of the normalised 112 calls by month steps. Is visible the increase of the involved municipalities respect to the March situation.

in Moldova

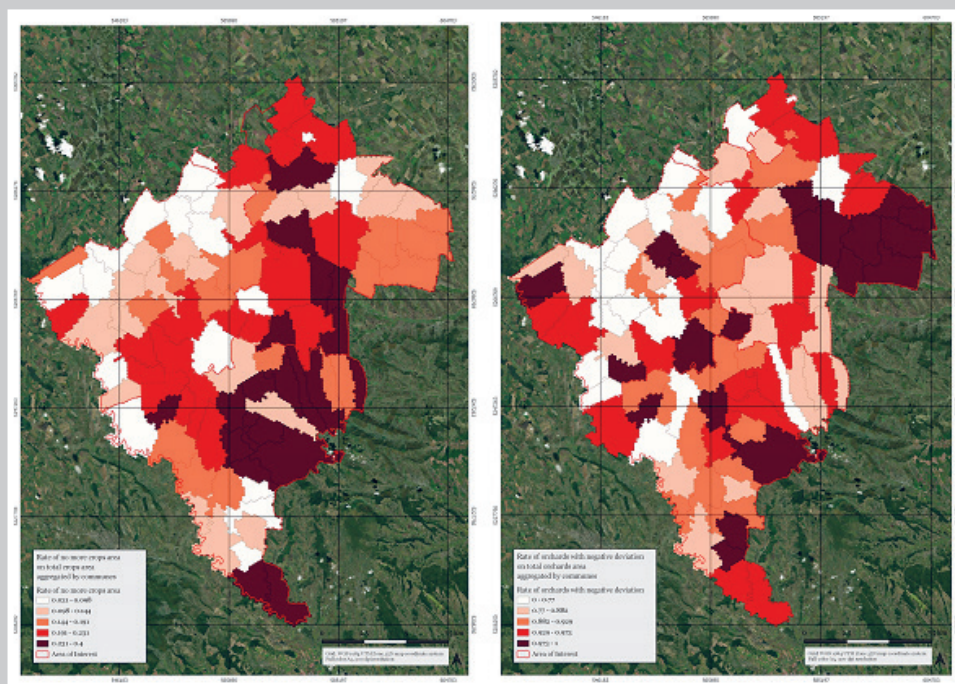
Figure 29: 112-emergency service calls registered as suspicious cases of Covid-19, normalised on population and classified by percentiles, and aggregated by municipalities.



The conclusive analysis is based on the inputs data given by the previous activities of Service 1 and 2. In order to highlight a possible correlation between 112-emergency calls and vegetation status, a system of scores has been applied.

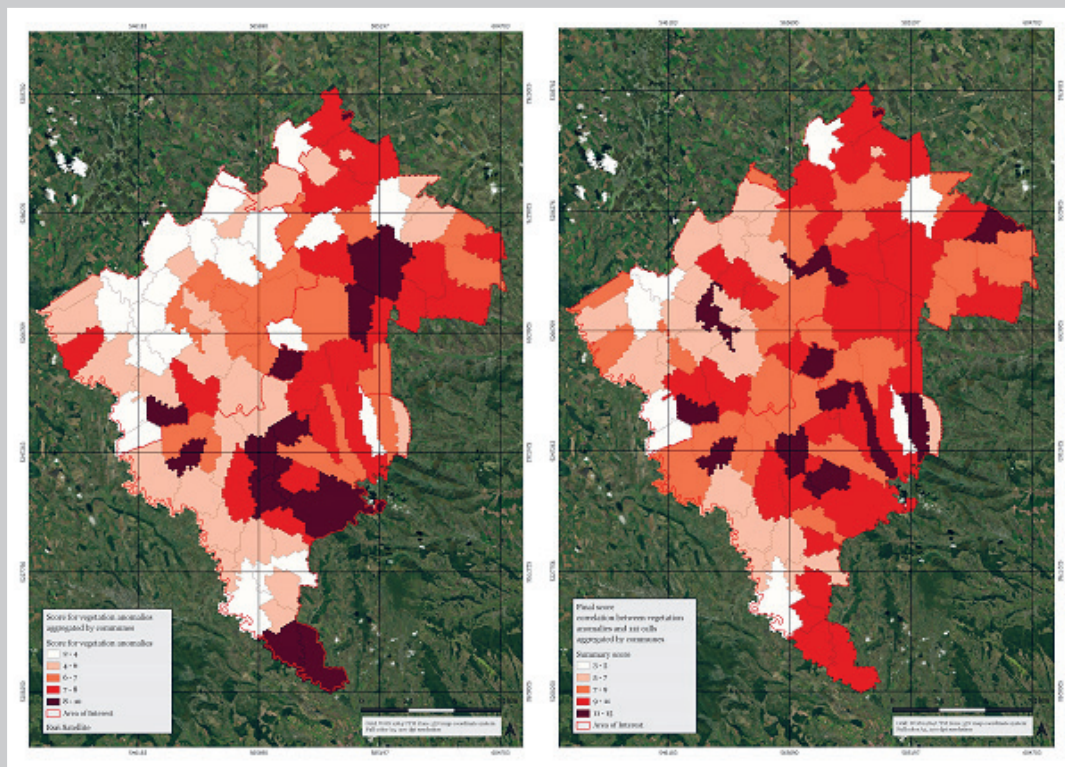
In the following figure, the rate of possible affected crops and orchards (no more visible in 2020 for the crops, with a negative deviation in 2020 for the orchards), respect to the total crops and orchards area is shown. Differences between outputs are quite evident and are mainly due to the different analysis applied to evaluate the vegetation status. In general, the Falesti district seems less affected respect to other rayons.

Figure 30: Distribution of the rate possible affected crops (left) and orchards (right), respect to the total crops and orchards area.



In the last figure it is shown on the left the cumulative index which take into account crops and orchards status, on the right the summary index, which shows area where vegetation anomalies and 112 emergency calls related to suspicious covid-19 cases have higher values. Results highlight a more critical situation in the Eastern municipalities, but only further analysis, can confirm the mapped events of this work.

Figure 31: On the left, the final score obtained to evaluate the general deviation of the vegetation status respect to the lasts years. On the right the summary index which aim to link the previous index with the one calculated for the 112-emergency calls analysed.



### 3.2.2 Quality Control and Validation

The quality control for service 2 was performed firstly on input data by verifying their usability, completeness and suitability for the purpose.

In particular, regarding the activity of mapping of 2020 vegetation status in AOI, checks were performed for the identification of orchards and for the mapping of vegetation status.

#### S2 completeness analysis over orchard areas

As far as the mapping of orchard vegetation status is concerned, the completeness of the time-series of input NDVI decadal and monthly composites derived from Sentinel-2 data was investigated with automatic procedures. In particular, temporal and spatial completeness were evaluated. As shown in following TABLE 6, the results of this quality control highlighted that no significant information gaps are present in the monthly dataset. Therefore, the NDVI time-series analysis can be performed on a monthly basis. As shown in the TABLE 7, the only critical period is observed in 2017, when only Sentinel-2A data were available in the first months of the year. In all other cases, most of the orchard areas in AOI presented at least 65% of good observations.

Quality layers (QA) were derived from the completeness analysis, providing for each year the number of good monthly observations in orchard areas. A maximum of 12 good observation in a year is expected. An example is provided in Figure 32.

Table 6: Percent area distribution of monthly good observations in orchard areas, during the period of analysis (Jan 2017-May 2020) - yearly analysis.

	Number of monthly good observations in a year, %												
	0	1	2	3	4	5	6	7	8	9	10	11	12
2017	0.00	0.00	0.00	0.00	0.00	0.00	0.06	2.14	13.24	37.09	37.69	9.34	0.44
2018	0.00	0.00	0.00	0.00	0.00	0.00	0.00	0.03	0.50	2.72	14.57	46.76	35.42
2019	0.00	0.00	0.00	0.00	0.00	0.00	0.00	0.26	3.50	13.63	28.00	33.28	21.31
2020	0.00	0.00	0.22	8.43	67.62	23.73	-	-	-	-	-	-	-

Table 7: Percent area distribution of monthly good observations in orchard areas, during the period of analysis (Jan 2017-May 2020) - monthly analysis.

	Number of monthly good observations in the considered years				
	0	1	2	3	4*
jan.	0.07%	1.40%	6.77%	<b>45.03%</b>	<b>46.73%</b>
feb.	3.61%	<b>39.89%</b>	<b>43.00%</b>	<b>10.99%</b>	2.50%
march	0.00%	0.04%	3.27%	<b>31.62%</b>	<b>65.07%</b>
apr.	0.00%	0.00%	<b>38.35%</b>	<b>61.65%</b>	0.00%
may	0.00%	0.03%	0.60%	<b>14.12%</b>	<b>85.24%</b>
jun.	0.00%	0.00%	0.19%	<b>99.81%</b>	-
jul.	0.00%	0.00%	0.21%	<b>99.79%</b>	-
aug.	0.00%	0.00%	0.00%	<b>100.00%</b>	-
sep.	0.00%	0.00%	0.00%	<b>100.00%</b>	-
oct.	0.00%	0.00%	0.06%	<b>99.94%</b>	-
nov.	1.34%	<b>25.80%</b>	<b>58.84%</b>	<b>14.02%</b>	-
dec.	1.77%	<b>14.77%</b>	<b>40.89%</b>	<b>42.57%</b>	-

\* maximum possible value of good observations only for the months ranging from January to May, for the remaining months 3 is the maximum value to be considered.



### Orchard map validation

Regarding the identification and mapping of orchard areas, two validation steps have been carried out: a visual inspection and refinement of the orchards extracted by means of computer-aided photo interpretation and a quantitative independent validation, based on a stratification approach.

The quantitative validation was performed in three steps:

1. sampling based on stratified sampling schema, in order to assure that sampled pixels/points are well distributed in the orchard classes and in the AOI;
2. independent photo-interpretation of sampled points;
3. computation of the error matrix for the sample points.

The adopted stratified random sampling schema aims at providing a number of sampling units proportional to the extent of the classes/strata of the orchard maps, including non orchard areas. The total number of sampled pixels was computed on the basis Olofsson et al. (2014)<sup>1</sup>, considering an expected minimum class user accuracy of 80% and standard error of the estimated overall accuracy to be achieved equal to 0.015.

The total number of sampled pixels *n* is distributed among the orchard classes of the map based on class map proportions of each class. A **minimum sample size of 50 pixels for each class**, in order to guarantee an acceptable standard error of the error estimates. For each class/stratum the number of pixels to be sampled is randomly extracted.

The number of sampled pixels was divided among the classes according to the TABLE 8.

Table 8: **Distribution of validation points.**

Class	Number of validation points
residential orchard	50
non residential orchard	73
non orchards	588

The overall accuracy identified with the validation is of 98.6% and can be considered suitable for the purposes of the analysis. The results of the validation process are reported in the confusion matrix in table 9.

The derived accuracies and errors obtained for the different classes are shown in Table 10, which shows high accuracies for all the considered classes. The obtained accuracies and errors can be considered suitable for the purposes of the analysis.

Table 9: **Confusion matrix.**

Classes		Reference			Total
		Residential orchard	Non residential orchard	Non orchard	
classified	residential orchard	49	0	1	50
	non residential orchard	0	71	2	73
	non orchard	4	3	581	588
	total	53	74	584	711

1. Olofsson, P., G.M. Foody, M. Herold, S.V. Stehman, Curtis E. Woodcock, Michael A. Wulder, (2014). Good practices for estimating area and assessing accuracy of land change, Remote Sensing of Environment, Volume 148, 25 May 2014, Pages 42-57, ISSN 0034-4257, <http://dx.doi.org/10.1016/j.rse.2014.02.015>.

Table 10: Classification accuracies and errors.

Class	User accuracy	Commission error	Producer accuracy	Omission error
Residential orchard	98.0%	2.0%	92.5%	7.5%
Non residential orchard	97.3%	2.7%	95.9%	4.1%
Non orchards	98.8%	1.2%	99.5%	0.5%

### Quality control for the ancillary data

For population data, the usability of the **GHSL data** is evaluated by comparing the data with the ones available at more aggregated spatial level for the 2019.

Looking at the table below, the change between 2015 and 2019 population is shown. Differences varies from negligible values to high ones (as for Balti municipality). These differences highlight as two datasets are not comparable (the variation is not uniform over the area).

Table 11: Population from 2019 and 2015 by rayon and variation between 2015 and 2019.

Admin. division	Population 2019 (Statistica Moldovei)	Population 2015 (GHSL)	Percent change 2015 - 2019, %
Balti	151 791	119 166	21.49
Falesti	90 275	93 780	-3.88
Singerei	91 412	90 794	0.68
Ungheni	116 705	105 038	10.00
<b>Moldova</b>	<b>3 542 708</b>	<b>3 555 159</b>	<b>-0.35</b>

Even if the accuracy of the dataset is not elevated, the GHSL has been chosen for the analysis, thanks to its better spatial resolution.

Another issue is related to the capability of the 112-emergency calls to provide a proxy for the description of the evolution of Covid-19 outbreak.

Looking at the general Covid-19 situation, numbers of cases are reported in ESRI online dashboard platform (based on the ArcGIS COVID-19 of John Hopkins). Looking at data of 05/07/2020, the 13,02% of national cases are reported in the AOI, which represent the 12,7 % of national population. In general, the rate of affected is 0.5% in the whole Moldova: urban areas have higher rates (0.92% for Balti municipality, 0,7% in Chisinau). In the following table, confirmed cases and population are compared. Looking at some general statistics, over around 13 500 calls in the time window in Moldova, about 15% are located in the area of interest (12% of national population). This data is obviously highly related to population, with high numbers in more populated areas. As from the table, rates have high variability (e.g. high number of calls in Ungheni respect to Covid-19 cases, and opposite situation in Balti), confirming that calls may be not a reliable proxy to describe Covid-19 spreads.

Table 12: Covid-19 cases from ESRI online dashboard platform of Moldova.

Admin. division	Confirmed cases	Population 2019	Covid-19 rate	Calls 112	Calls 112 rate	Calls on confirmed cases
Balti	1 401	151 791	0.92%	980	0.65%	69.95%
Falesti	380	90 275	0.42%	450	0.50%	118.42%
Singerei	425	91 412	0.46%	321	0.35%	75.53%
Ungheni	113	116 705	0.10%	269	0.23%	238.05%
<b>Moldova</b>	<b>17 814</b>	<b>3 542 708</b>	<b>0.50%</b>	<b>13 680</b>	<b>0.39%</b>	<b>76.79%</b>

As no other information with this level of spatial resolution where available on the area to describe the Covid-19, the work has been oriented only by these data.

### 3.2.3 Usage, Limitations and Constraints

In order to quantify the condition of the present 2020 orchard growing season and therefore to extract proposed phenological parameters, only Sentinel-2 imagery acquired up to May 2020 were available at the beginning of the present study. In the methodology adopted for this study, fitting operations of incomplete yearly NDVI function during the growing season and before its conclusion, and subsequent estimation of phenological parameters, are performed starting from an estimate of the seasonal NDVI function extracted from the historical normal one (evaluated using 2017-2019 Sentinel-2 imagery). The latter is adjusted by considering the deviations observed for the most updated available monthly NDVI values. In this way, this approach allows to profit of the benefits that the analysis of phenology for the identification of 2020 vegetation anomalous conditions guarantees, first of all the significant reduction of cloud contamination of base imagery, due to the adopted gap filling and fitting operations. Nevertheless, a reduced reliability could affect 2020 growing season phenological parameter extraction.

Proposed maps and data describing 2020 vegetation conditions and deviations are based on the analysis of phenological parameters extracted from satellite-derived datasets through a modelling process that requires making assumptions and user setting of some parameters. For these reasons, the description of vegetation growing season obtained using these parameters may not be completely consistent with development phases registered in phenological calendars commonly adopted in the agricultural sector and with actual yield values observed during the season. Moreover, this is of particular relevance for orchard areas, where the agricultural production is not clearly identifiable starting from measured plant biomass and vigor. However, the observed phenological parameters can be effectively used to compare vegetation conditions in different years and to identify, in particular, the areas where fruit trees evolution in 2020 show some modifications respect to 2017-2019 previous seasons, considered as reference conditions. Finally, cloud coverage affecting satellite optical acquisitions limits the temporal and spatial completeness of used NDVI time-series, as described in 3.2.2, particularly in the first and last months of the year, where residual information gaps are present in the used NDVI time-series. As a consequence a reduction of the final accuracy of modelling operations is expected.

Results obtained for demonstrating the spatial correlation between vegetational anomalies and Covid-19 impact must be considered as a first tentative to identify critical area. The choice to aggregate data on municipalities allows to maintain an adequate level of detail in the analysis and to link agricultural areas and residential area, on the assumption

that agricultural areas in a municipality were cultivated by the inhabitants of the same municipality. This simplification has been necessary because no other information about people movements in the area was available. Most of the limits of the analysis are related to the issues already cited in 3.2.3 chapter.

### 3.3 WEBGIS publication

All the outputs of project's activities are loaded on a Web-GIS platform, allowing the user to visualization and consultation of data.

This is the list of the available products loaded in the Web-GIS (a total of 73 products):

- **Orchards Layers (one raw layer and one statistics for each of years in 2017-2020 and a deviation layer)**
  - Start of Season
  - Mid Season
  - Length
  - Amplitude
- **Administrative Stats**
  - Call to 112
  - Vegetation and Orchards
- **Agricultural layers (one raw layer for each of years in 2017-2019):**
  - ConfCropMasked
  - CropMask
  - SeasonEndMasked
  - SeasonStartMasked
- **Agricultural layers (one raw layer for each of years in 2019-2020):**
  - MaxGreennessMasked
  - SeasonPeakMasked

The Web-GIS is available at: <http://witness-dev.egeos-services.it/mapstore/#/viewer/openlayers/72>

This is the screenshot of the interface:

